https://www.youtube.com/watch?v=paQFaQj15Uc

https://www.youtube.com/watch?v=jJay36_ojVE

https://www.youtube.com/watch?v=HcGKie1RG98

Observations & Interpretations

Tohoku-Aki 2011 Earthquake
The Cascadia Subduction Zone
Large Cascadia Earthquakes
The 1700 Cascadia Quake
Vertical Motions in Cascadia
Quaternary stratigraphy of coastal estuaries
Offshore Cascadia fore-arc deformation
Tremor and episodic slip in Cascadia
Portland Earthquake Hazards

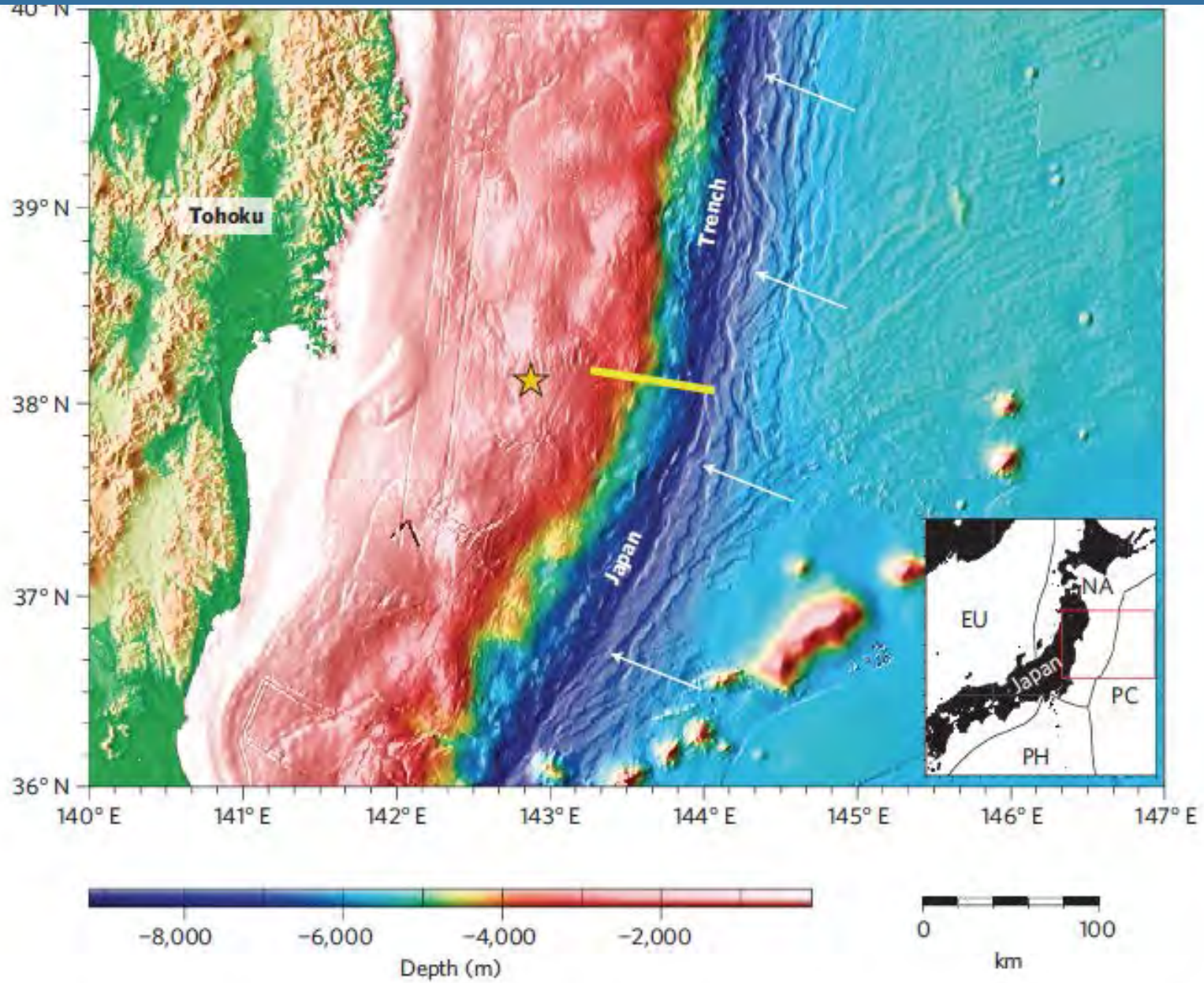

Figure 1 | Map showing the location of the seismic profile. The yellow line and star indicate the profile studied here and the epicentre of the 2011 Tohoku-oki earthquake determined by the Japan Meteorological Agency, respectively. White arrows indicate the relative motion of the Pacific plate, holding the Japan mainland fixed[6]. PC, Pacific plate; NA, North America plate; EU, Eurasia plate; PH, Philippine Sea plate.

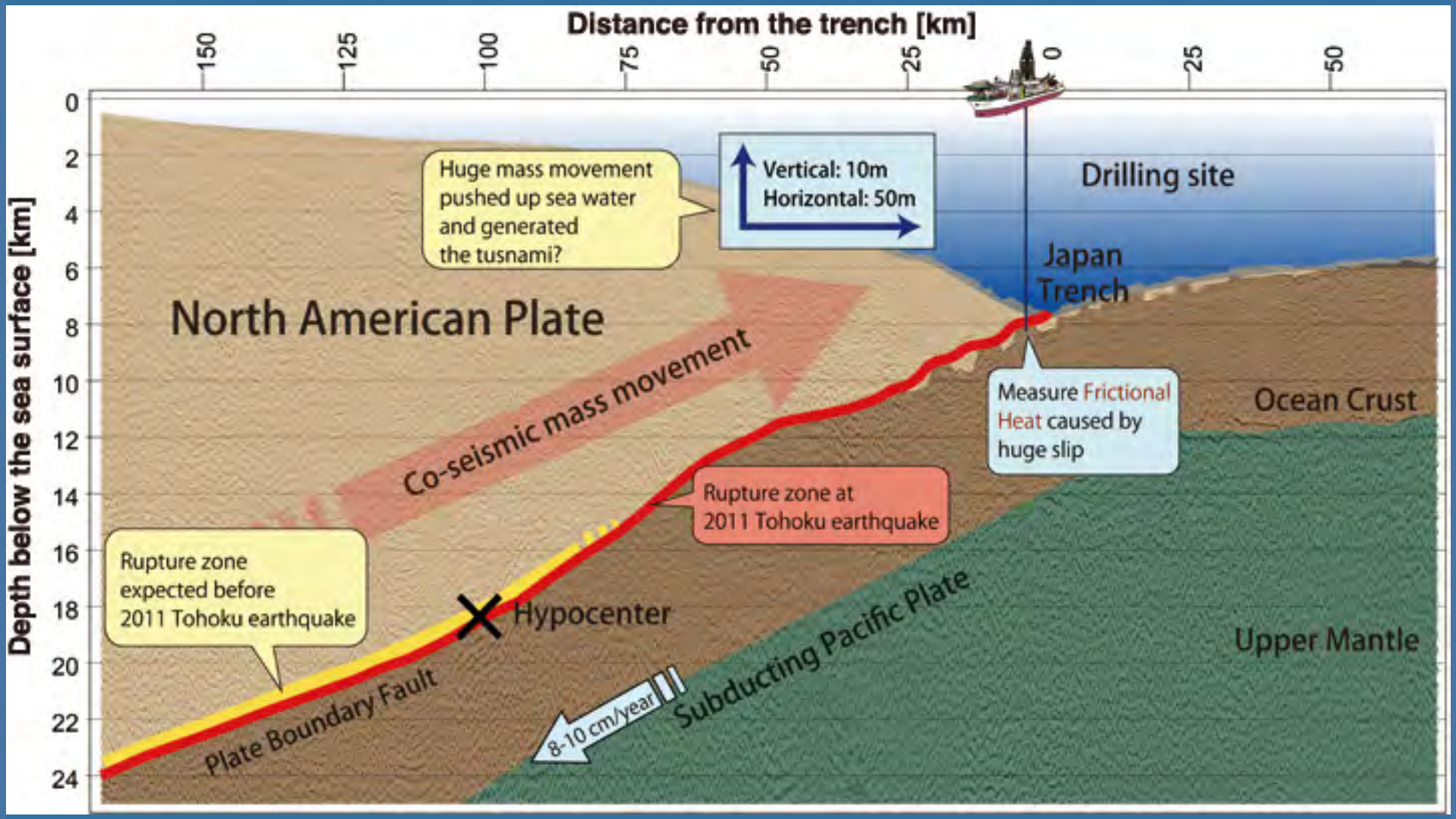

http-//www.jamstec.go.jp/chikyu/magazine/e/special/no13/img/pic05_up.jpg

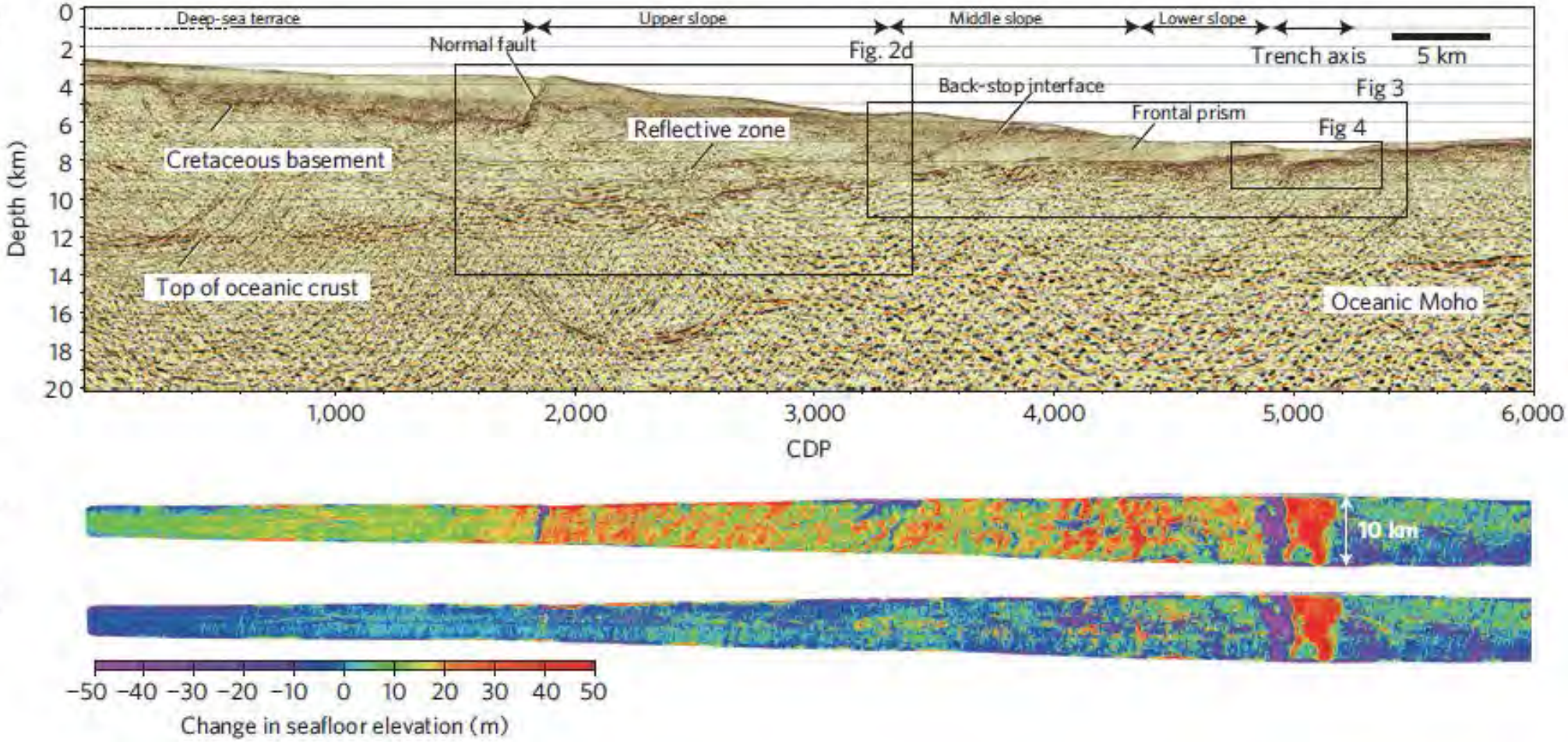

Figure 2 | Seismic reflection and differential bathymetry image seawards of the epicentre. a, Seismic reflection section obtained in 2011. No vertical exaggeration. CDP, common depth point (no unit). **b**, Differential bathymetry image between the bathymetric data acquired in 1999 and the data acquired after the earthquake. **c**, Differential bathymetry image between the 1999 data and the data transformed by shifting the bathymetry obtained after the earthquake horizontally landwards by 50 m and downwards by 10 m. The resolution of the bathymetry data is discussed in detail in ref. 11. **d**, Enlarged seismic section of the reflective zone beneath the upper slope (within the rectangle shown in **a**). Black arrows indicate landward-dipping normal faults.

Kodaira et al 2012

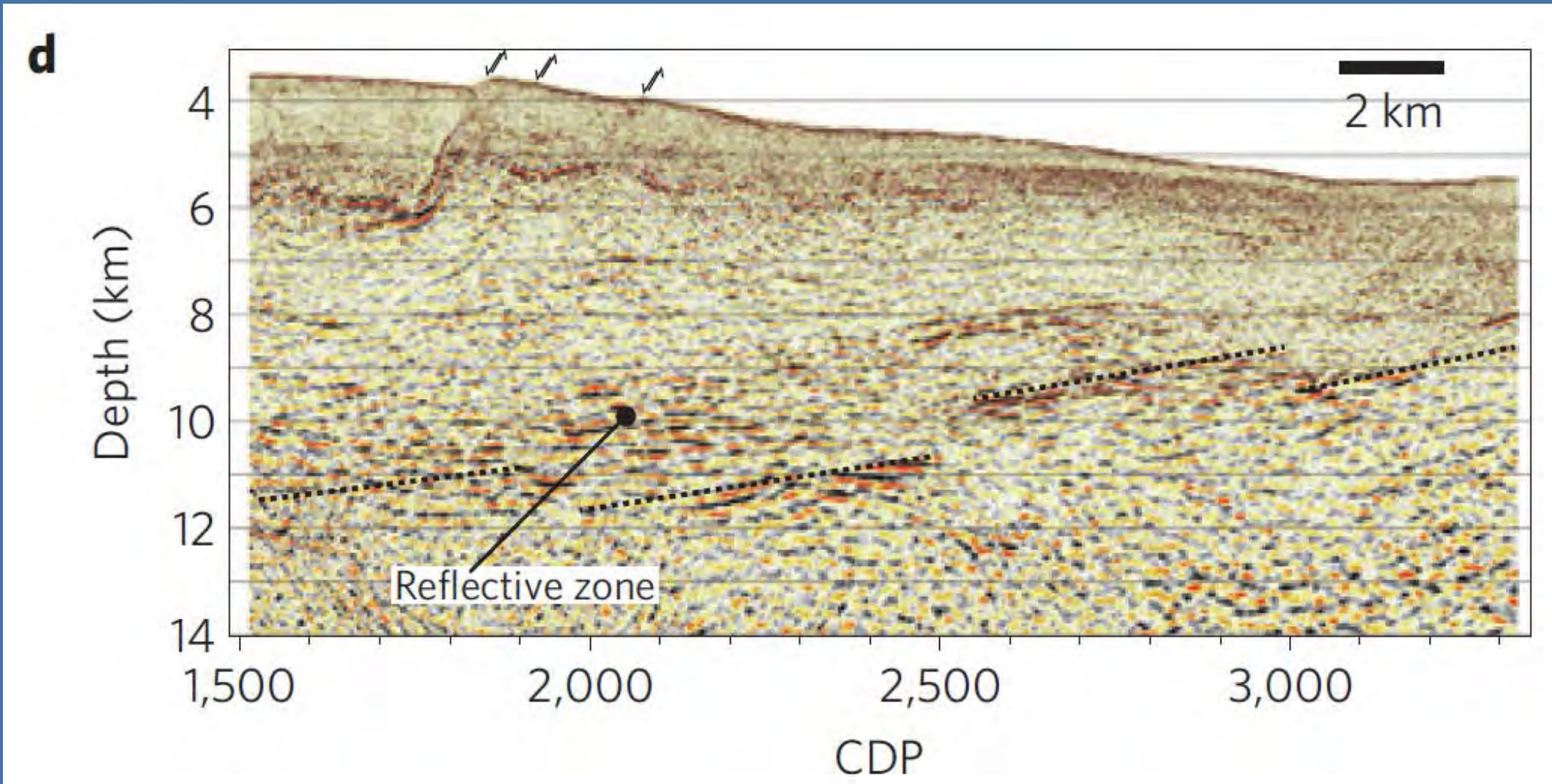

Figure 2 | Seismic reflection and differential bathymetry image seawards of the epicentre. a, Seismic reflection section obtained in 2011. No vertical exaggeration. CDP, common depth point (no unit). **b**, Differential bathymetry image between the bathymetric data acquired in 1999 and the data acquired after the earthquake. **c**, Differential bathymetry image between the 1999 data and the data transformed by shifting the bathymetry obtained after the earthquake horizontally landwards by 50 m and downwards by 10 m. The resolution of the bathymetry data is discussed in detail in ref. 11. **d**, Enlarged seismic section of the reflective zone beneath the upper slope (within the rectangle shown in **a**). Black arrows indicate landward-dipping normal faults.

Kodaira et al 2012

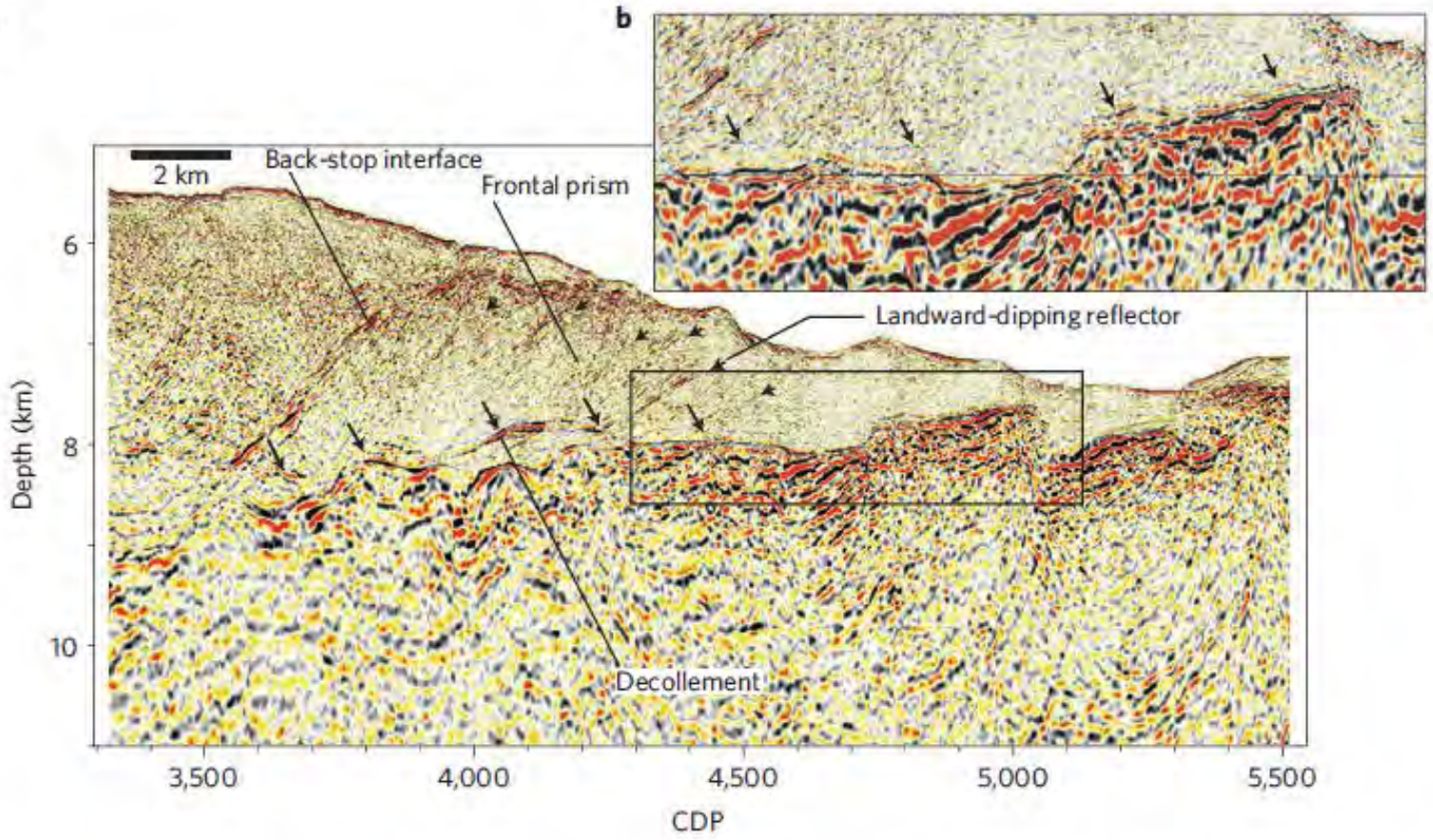

Figure 3 | Seismic image of the frontal prism. a, Enlarged seismic image of the frontal prism (location shown in Fig. 2a) obtained in 2011. Vertical exaggeration, 2:1. **b**, Enlarged section of the area outlined in **a**. Large arrows (**a**,**b**) indicate a reflector interpreted as the decollement interface. Smaller, shallow arrows in **a** indicate landward-dipping reflectors in the frontal prism.

Kodaira et al 2012

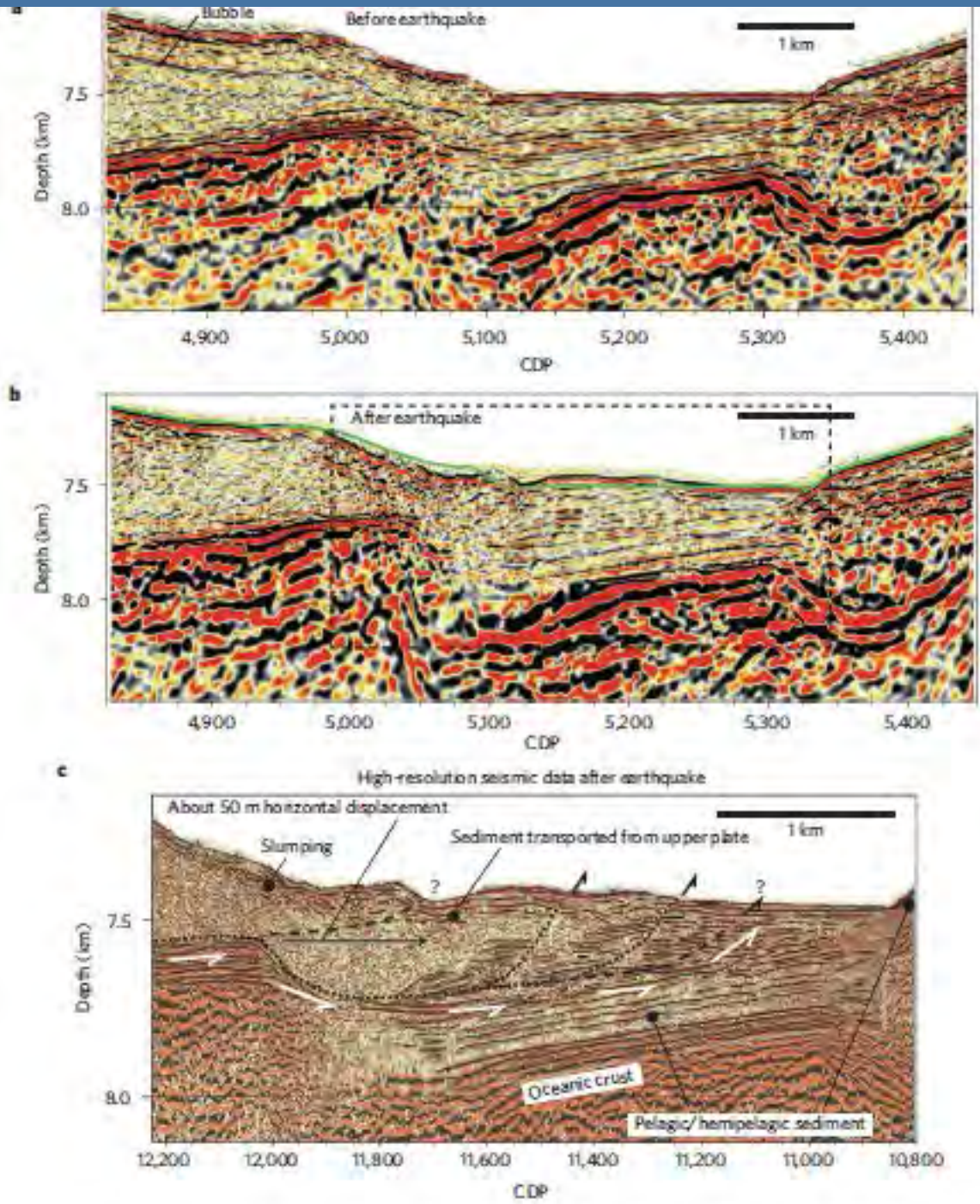

Figure 4 | Comparison of seismic images obtained before and after the earthquake. a, Seismic image of the trench axis obtained in 2009 before the earthquake. An interface imaged ~200 m below the sea floor (black interface) at the landward slope of the trench is an artefact generated by a bubble signal from a non-tuned large airgun. Vertical exaggeration, 2:1. **b**, Seismic image of the trench axis obtained after the earthquake. Vertical exaggeration, 2:1. Green line indicates the sea floor before the earthquake. **c**, Interpretation of the high-resolution seismic image obtained after the earthquake around the trench (within the rectangle shown in **b**). See also Supplementary Information.

Kodaira et al 2012

Aeromag & EQ Model of Cascadia Subduction Zone

- Parsons et al (1998)
- A new view into the Cascadia subduction zone and volcanic arc: Implications for earthquake hazards along the Washington Margin
- Geology v 26 pp 199-202.

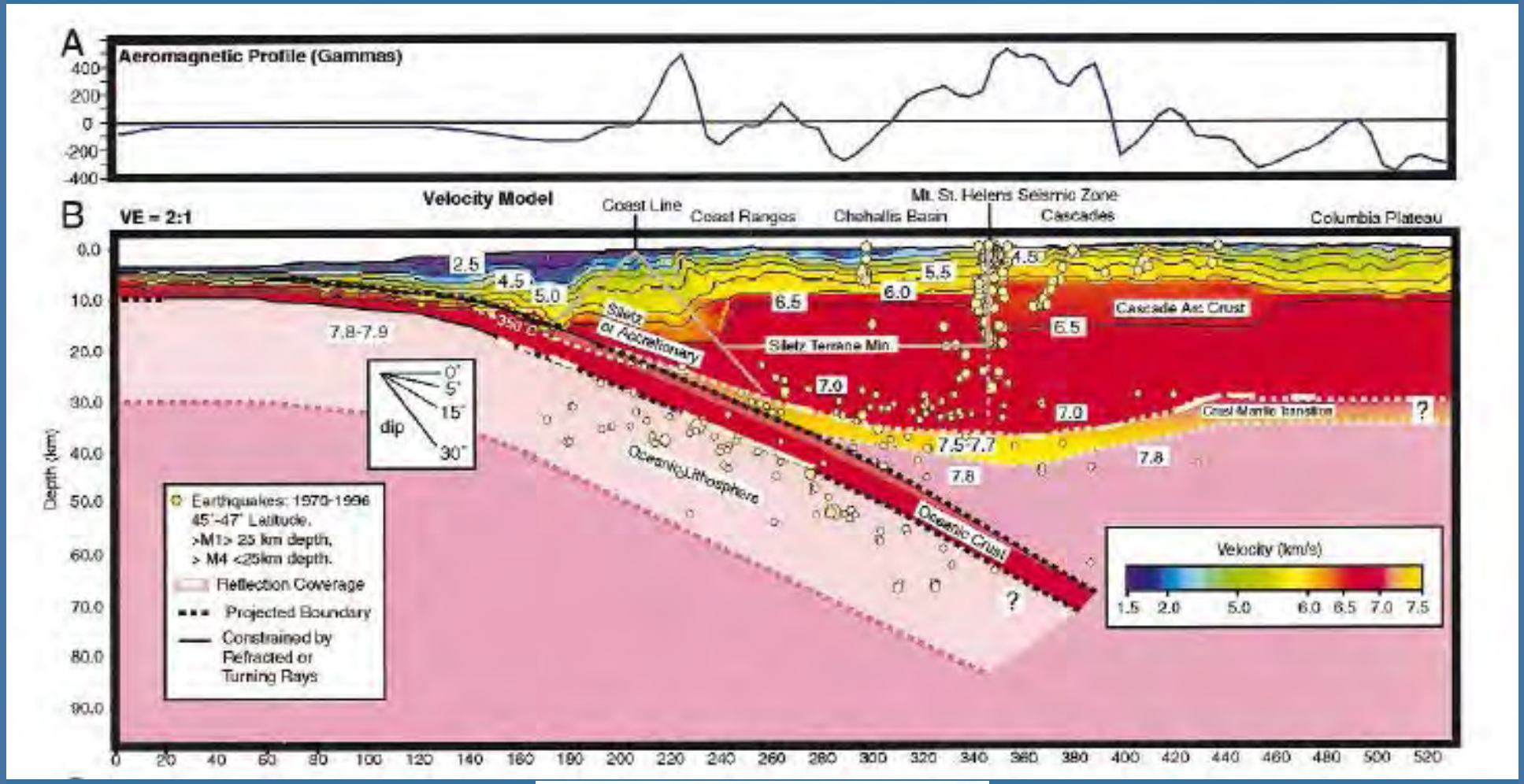
A
Aeromagnetic Profile (Gammas)
400
200
0
-200
-400
B
VE = 2:1
Velocity Model
Coast Line
Coast Ranges
Chehalis Basin
Mt. St. Helens Seismic Zone
Cascades
Columbia Plateau
Depth (km)
2.5
4.5
5.0
6.5
6.0
5.5
4.5
7.8-7.9
Siletz or Accretionary
Siletz Terrane Mtn.
Cascade Arc Crust
7.0
7.0
Crust-Mantle Transition
?
7.5-7.7
7.8
7.8
Oceanic Lithosphere
Oceanic Crust
dip
0°
5°
15°
30°
Earthquakes: 1970-1996
45°-47° Latitude,
>M1< 25 km depth,
> M4 <25km depth.
Reflection Coverage
Projected Boundary
Constrained by Refracted or Turning Rays
Velocity (km/s)
1.5 2.0 5.0 6.0 6.5 7.0 7.5
0 20 40 60 80 100 120 140 160 180 200 220 240 260 280 300 320 340 360 380 400 420 440 460 480 500 520

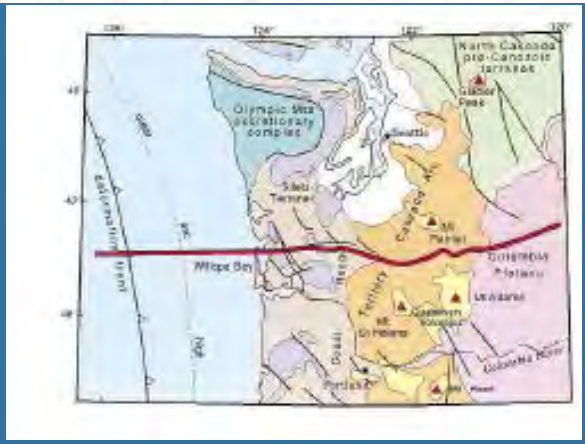

Large Earthquakes in Cascadia

- Clagg (1997)
- Evidence for large earthquakes at the Cascadia subduction zone
- Reviews of Geophysics v 35 pp 439-460.

Cascadia Soils: The Story They Tell

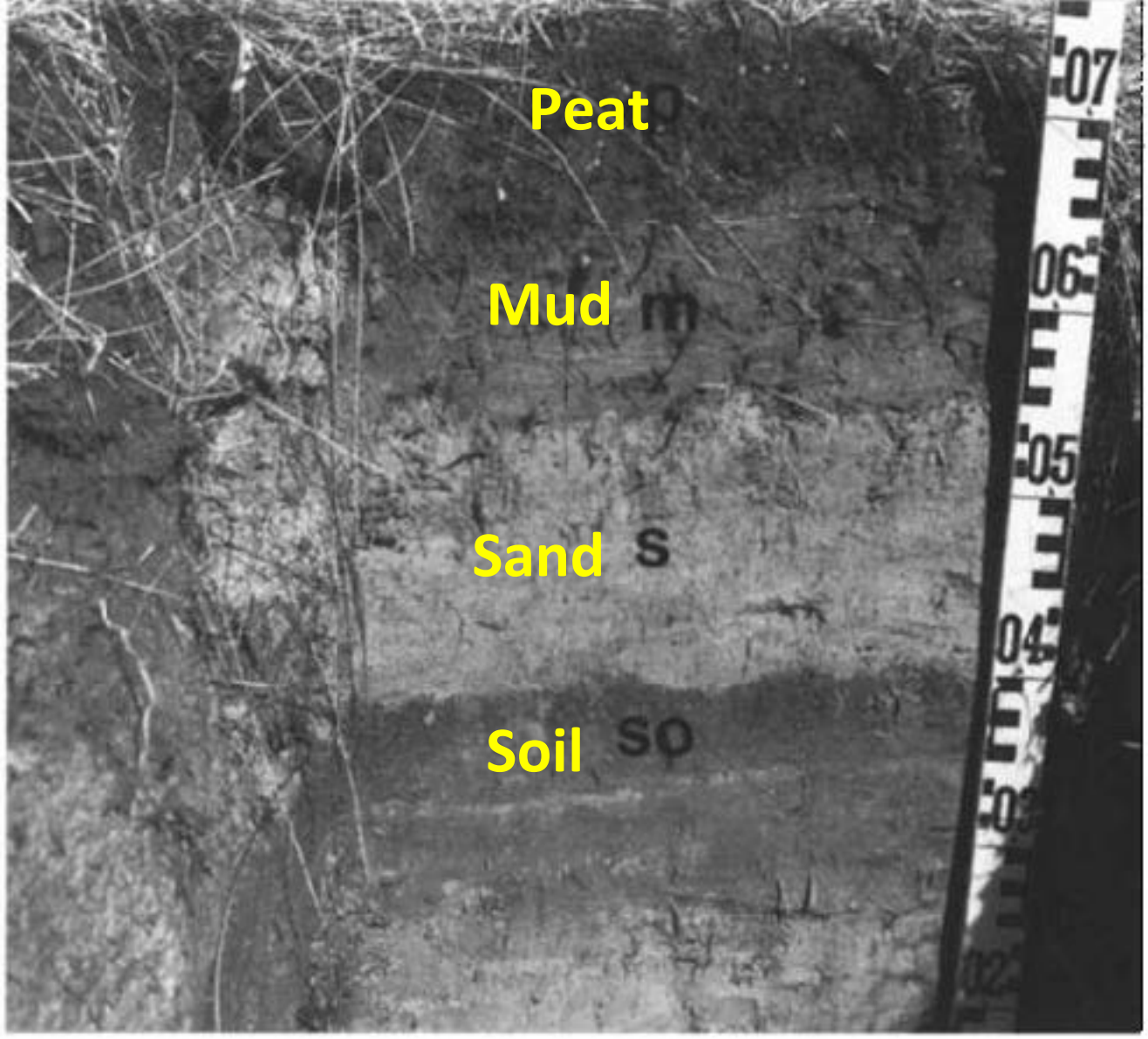

Figure 9. Tsunami sand (labeled s) overlying an eroded peaty soil (so) in a pit dug near Tofino, British Columbia (photo by J. J. Clague). The tsunami was triggered by a large earthquake about 300 years ago. The sand is overlain by intertidal mud (m) which grades upward into peat (p) of the present-day marsh. The smallest divisions on the stadia rod are centimeters.

Clagg 1997

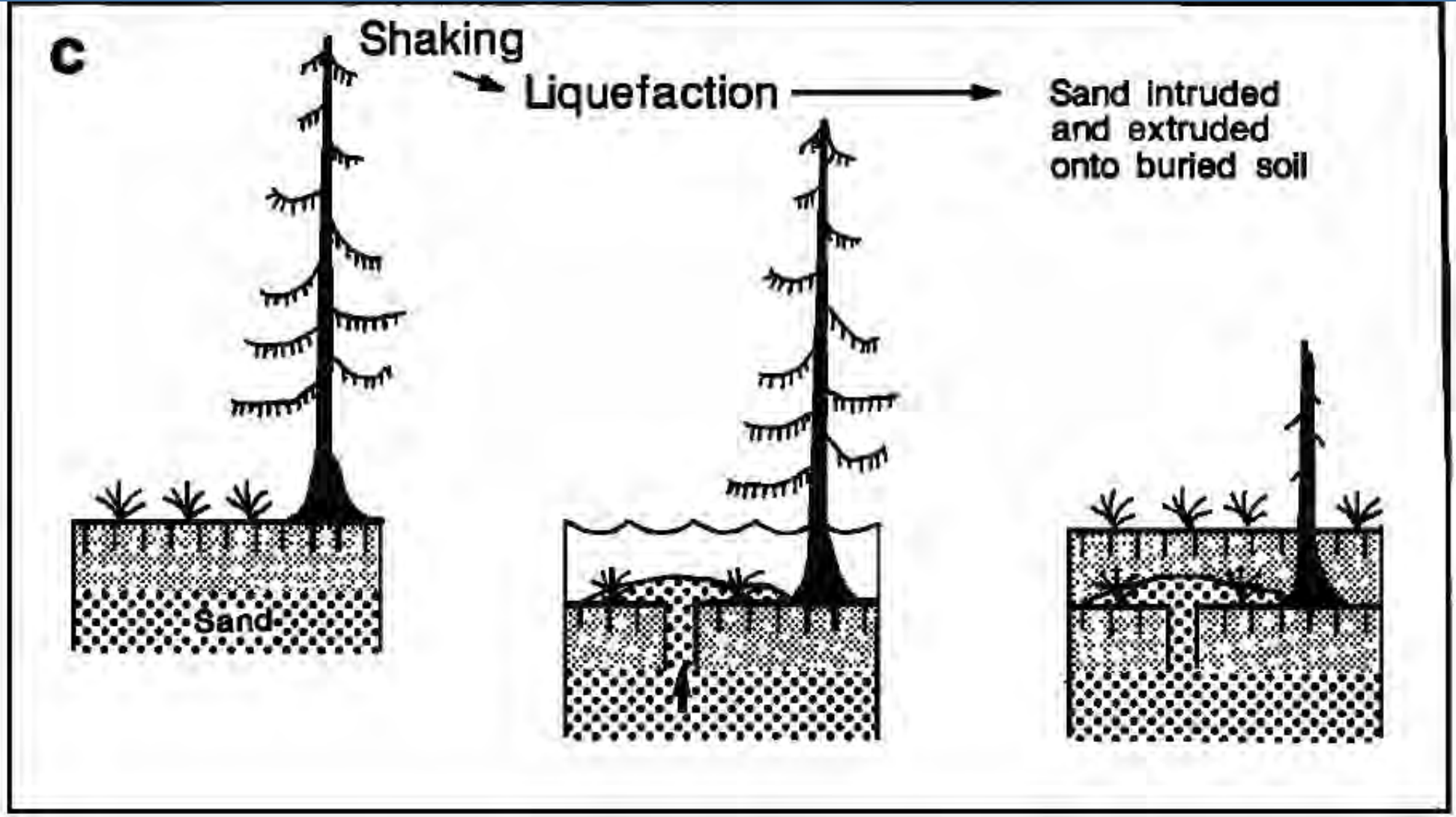

Figure 7. Simplified diagrams showing origins of coastal geological evidence for large Cascadian plate boundary earthquakes (modified from *Atwater et al.* [1995, Figure 3] with permission from the Earthquake Engineering Research Institute). (a) A marsh subsides into the intertidal zone during an earthquake and is buried by mud. (b) A tsunami deposits sand on a coseismically subsided surface. (c) Liquefied sand moves upward through cohesive sediment and spills onto a coseismically subsided surface.

Clagg 1997

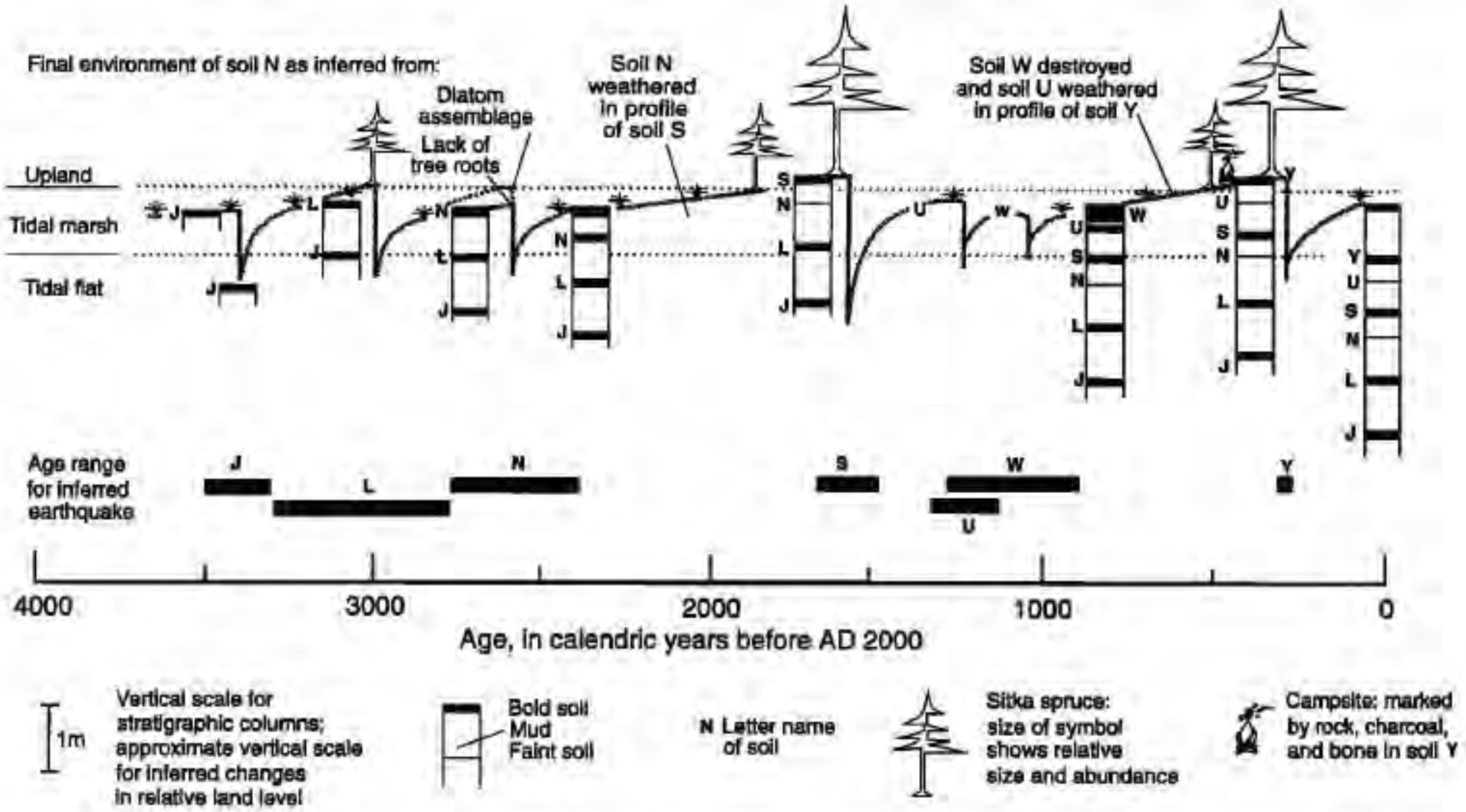

Figure 10. Diagrammatic representation of land level, vegetation, and soil changes at an estuary in southwestern Washington where there is evidence for seven large earthquakes in the last 4000 years (modified from *Atwater and Hemphill-Haley* [1996, Figure 15]). Each buried soil, shown as a lettered horizontal line in the stratigraphic columns, records an earthquake that caused at least 0.5 m of subsidence. Soils are separated by silty and clayey sediments deposited between earthquakes. The age ranges of the earthquakes are based on radiocarbon ages.

Clagg 1997

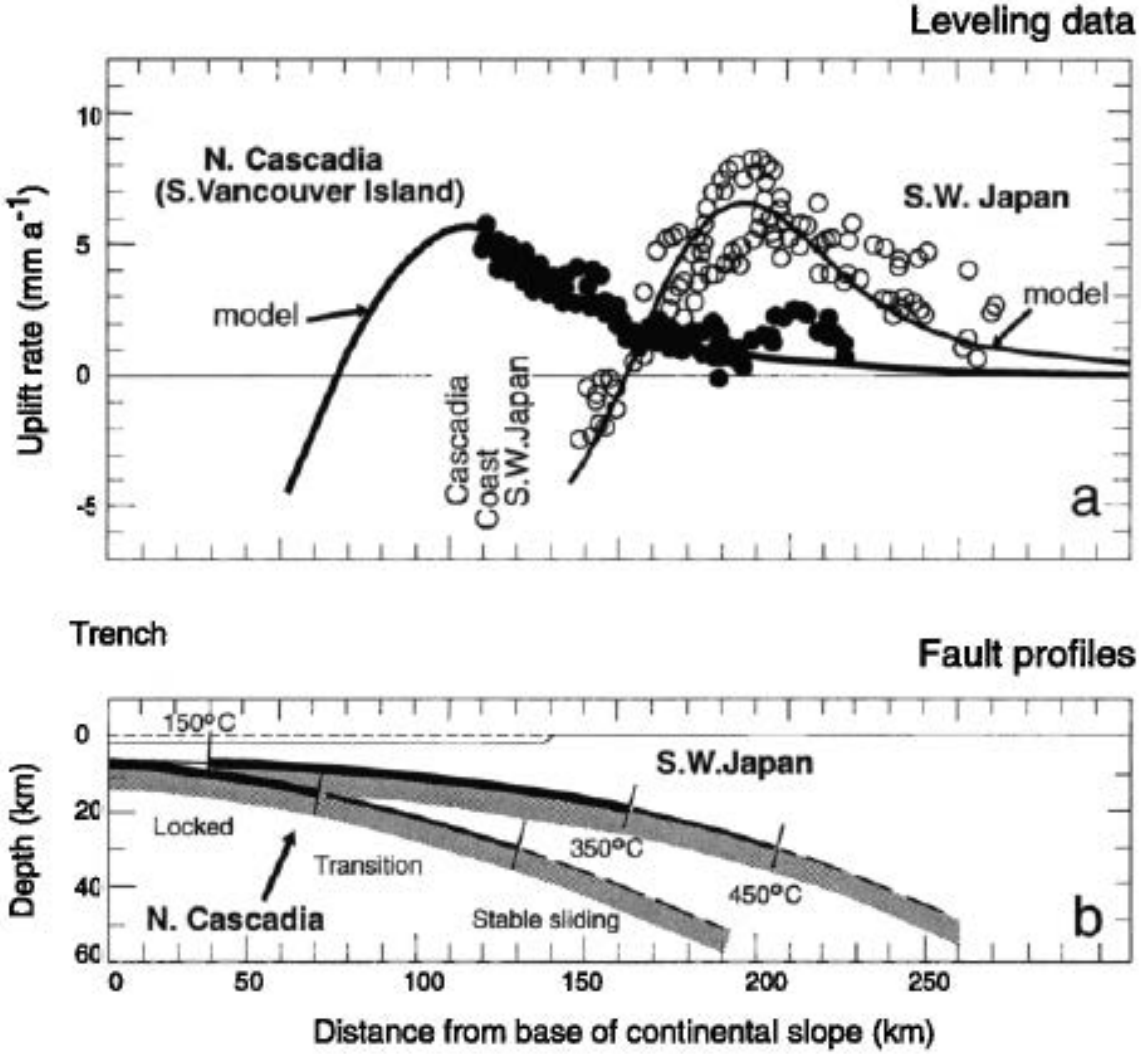

Figure 4. (a) Uplift of coastal regions of northern Cascadia and southwest Japan as determined from repeated leveling surveys (symbols) and as predicted for the temperature-controlled zones shown in Figure 4b (curves). (b) Profiles showing locked (<150°C), transition (150°–350°C), and stable sliding (>450°C) zones, corresponding to model curves in Figure 4a. Note that the flexural bulge and inferred lock zone extend farther landward in Japan than in Cascadia. (Modified from *Hyndman and Wang* [1995, Figure 16]).

Clagg 1997

The 1700 Cascadia Quake

Leonard, Hyndman and Mazotti 2001
Coseismic subsidence in the 1700 great Cascadia eathquake: Coastal estimates versus elastic dislocation models

GSA Bulletin pp 655-670 pp 655-670

Figure 1. Plate tectonic setting of the Cascadia subduction zone

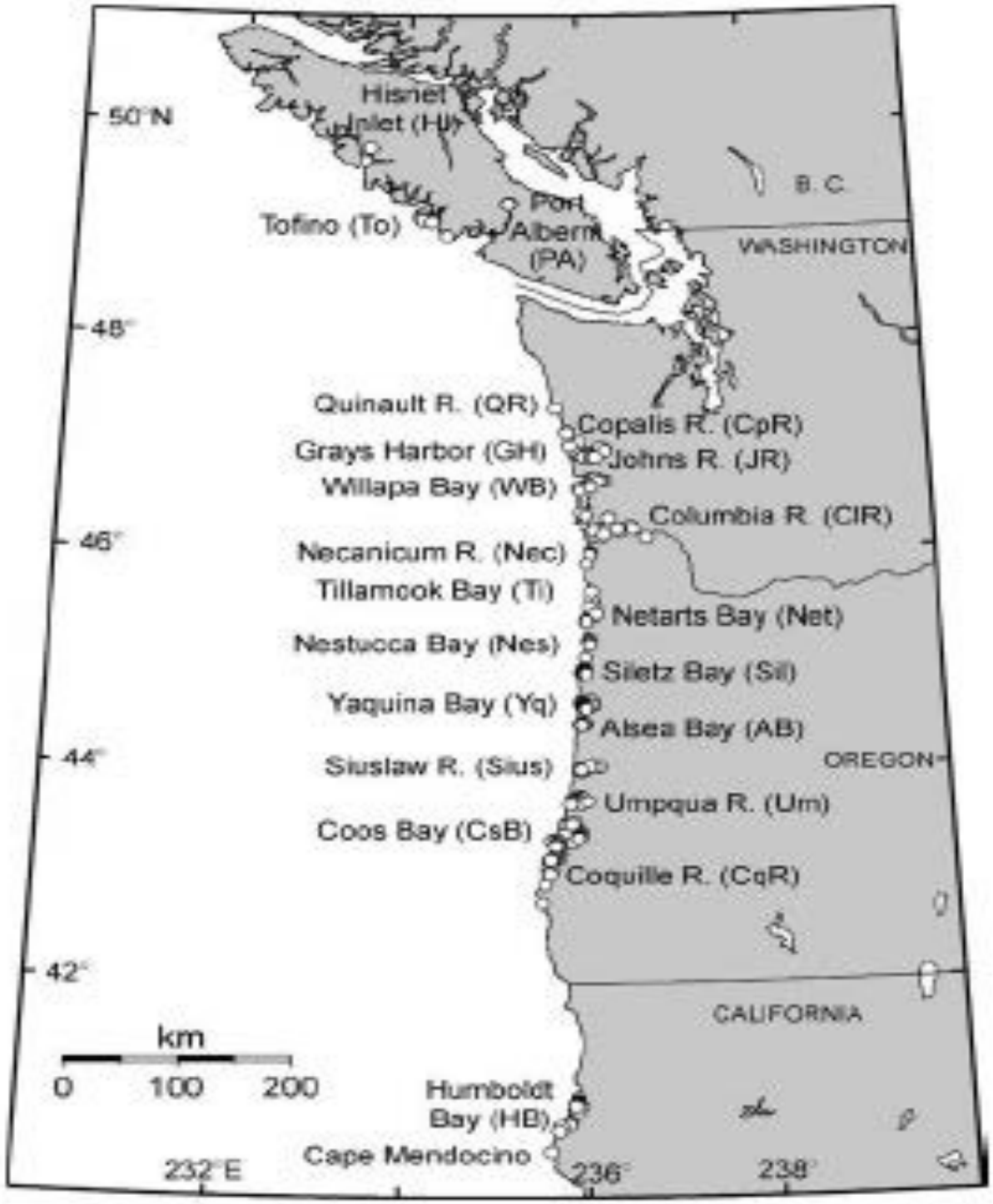

Figure 4. Location of Cascadia estuaries from which subsidence data have been extracted. Open circles mark data sites.

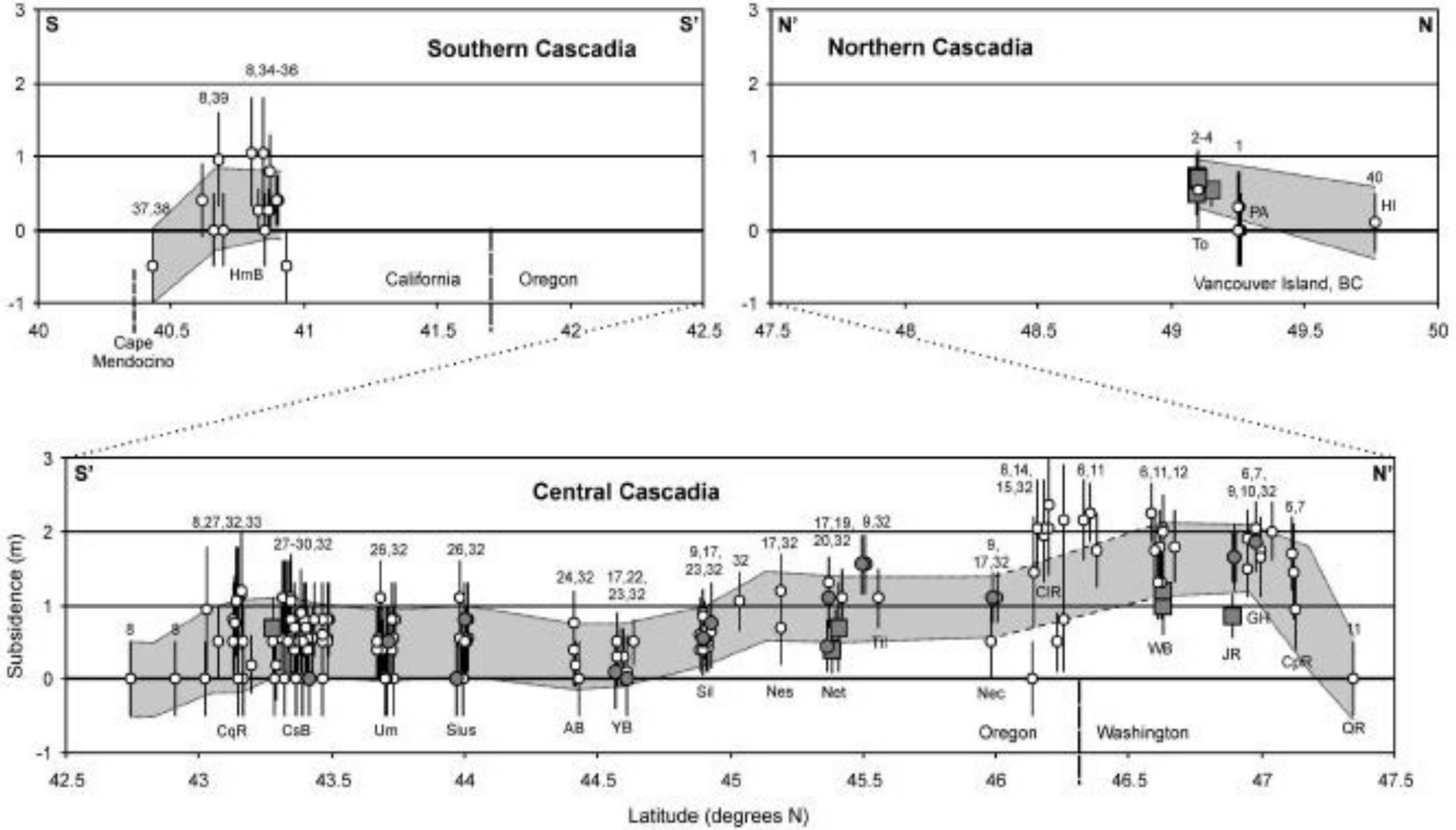

Figure 6. Compilation of coseismic subsidence estimates made using method 1, plotted against latitude. Individual error bars represent uncertainty due to range of possible paleoelevations above and below 1700 horizon. Gray shading represents weighted mean plus or minus weighted standard deviation of groups of points; Columbia River and Port Alberni data are excluded from this shading, the former due to unreliability as discussed in text, the latter due to location significantly inland. Gray squares are estimates made via detailed microfossil studies; gray circles represent estimates made using organic content and relative percentage of freshwater/brackish diatoms plus or minus plant macrofossils; open circles are estimates made using organic content plus or minus plant macrofossils. Locations and abbreviations are shown in Figure 4. Numbers above data points reference data sources (see Table 1).

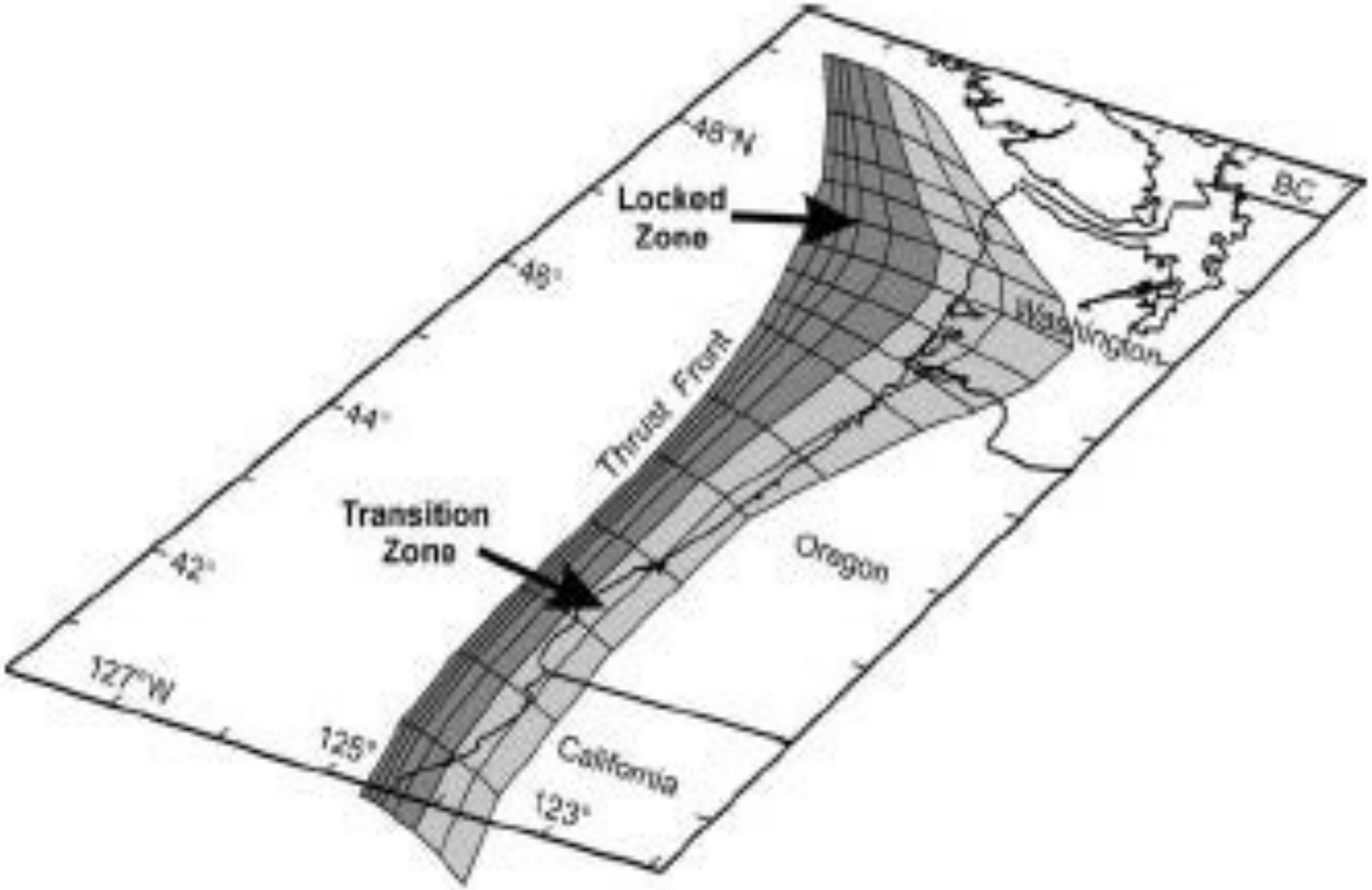

Figure 8. Locked and transition zones of Cascadia megathrust (based on thermal constraints and geodetic data) used in elastic dislocation model (after Flück et al., 1997).

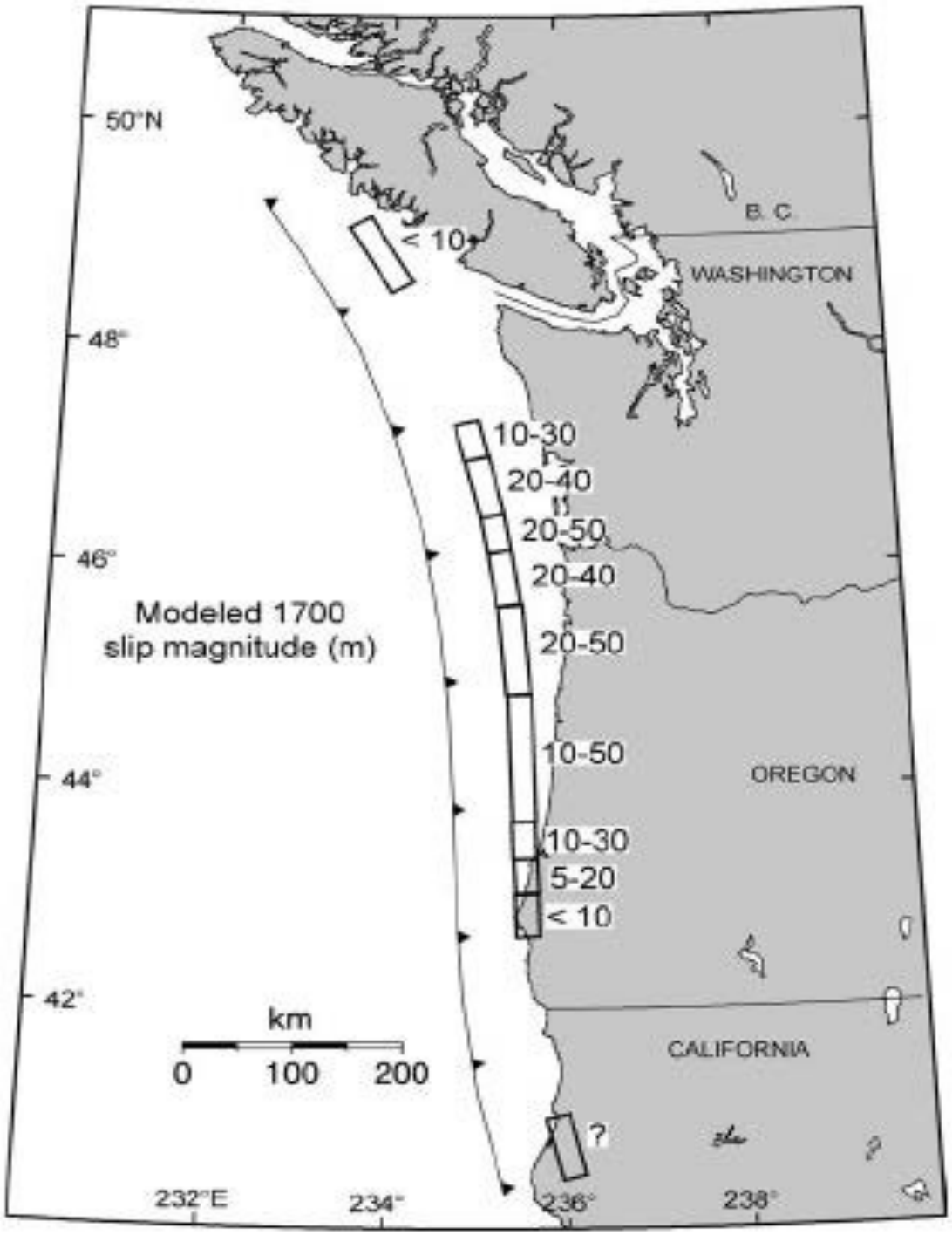

Figure 11. Along-coast variations in slip magnitude for 1700 earthquake, from comparisons of predictions of elastic dislocation uniform slip models with geological subsidence estimates (Fig. 9B). Plate convergence over 800 yr ranges, north to south, from 22 to 36 m.

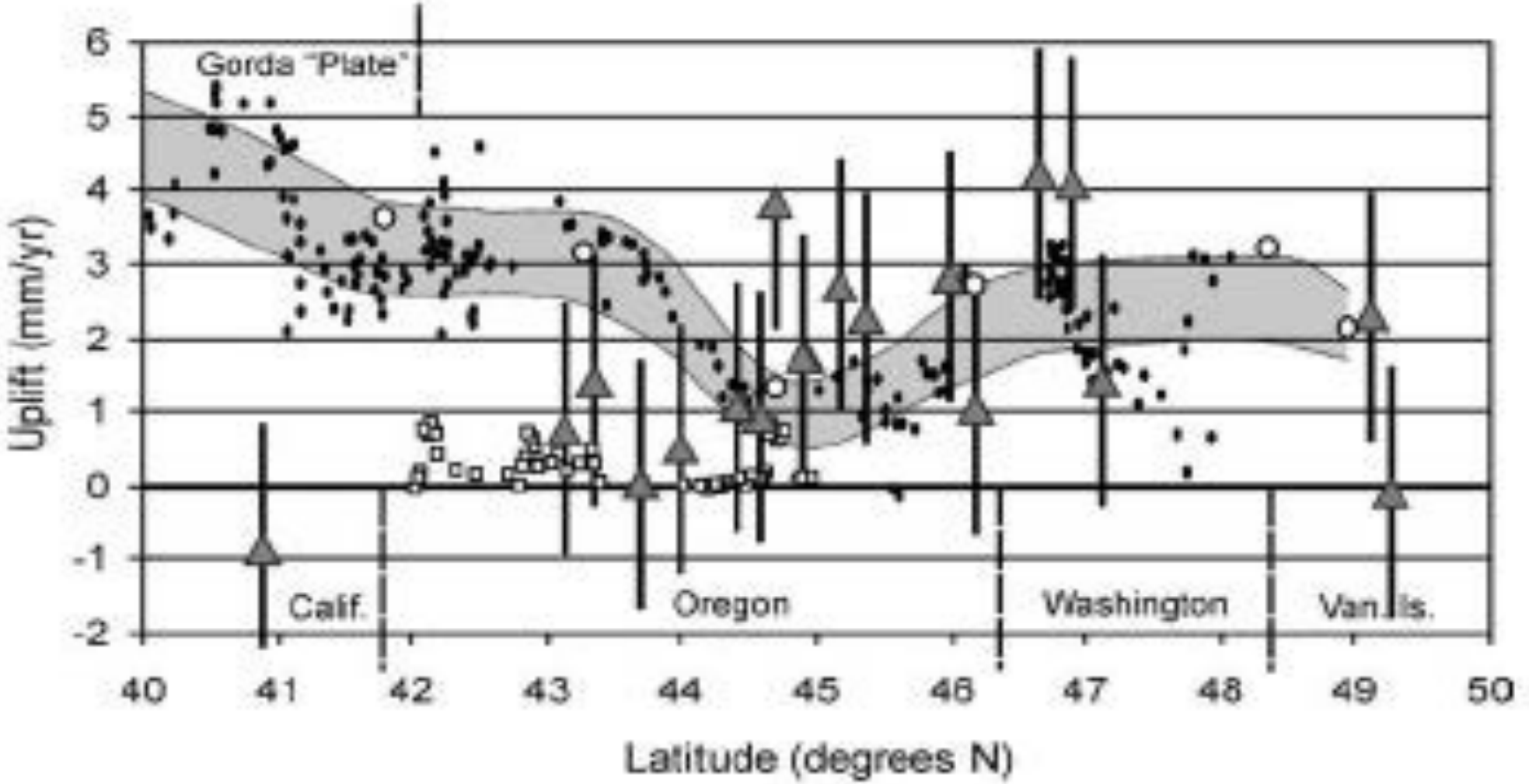

Figure 14. Interseismic uplift since 1700 (gray triangles) calculated inversely using method shown in Figure 12 (method 2) and converted to millimeters per year, compared with recent geodetic measurements of uplift (open circles, tide gauge data; filled circles, leveling data; shaded curve represents ~1σ of geodetic data; Hyndman and Wang, 1995) and long-term uplift estimates based on uplifted shore platforms of 80, 105, and 125 ka (open squares; Kelsey et al., 1994). Error bars are based on assumed error of subsidence estimates of ± 0.5 m. Calif.—California; Van. Is.—Vancouver Island.

Central Oregon Coast Estuaries

Witter et al (2003)

Great Cascadia earthquakes and tsunamis of the past 6700 years, Coquille river estuary, southern Coastal Oregon

GSA BulleOn pp 1289–1306

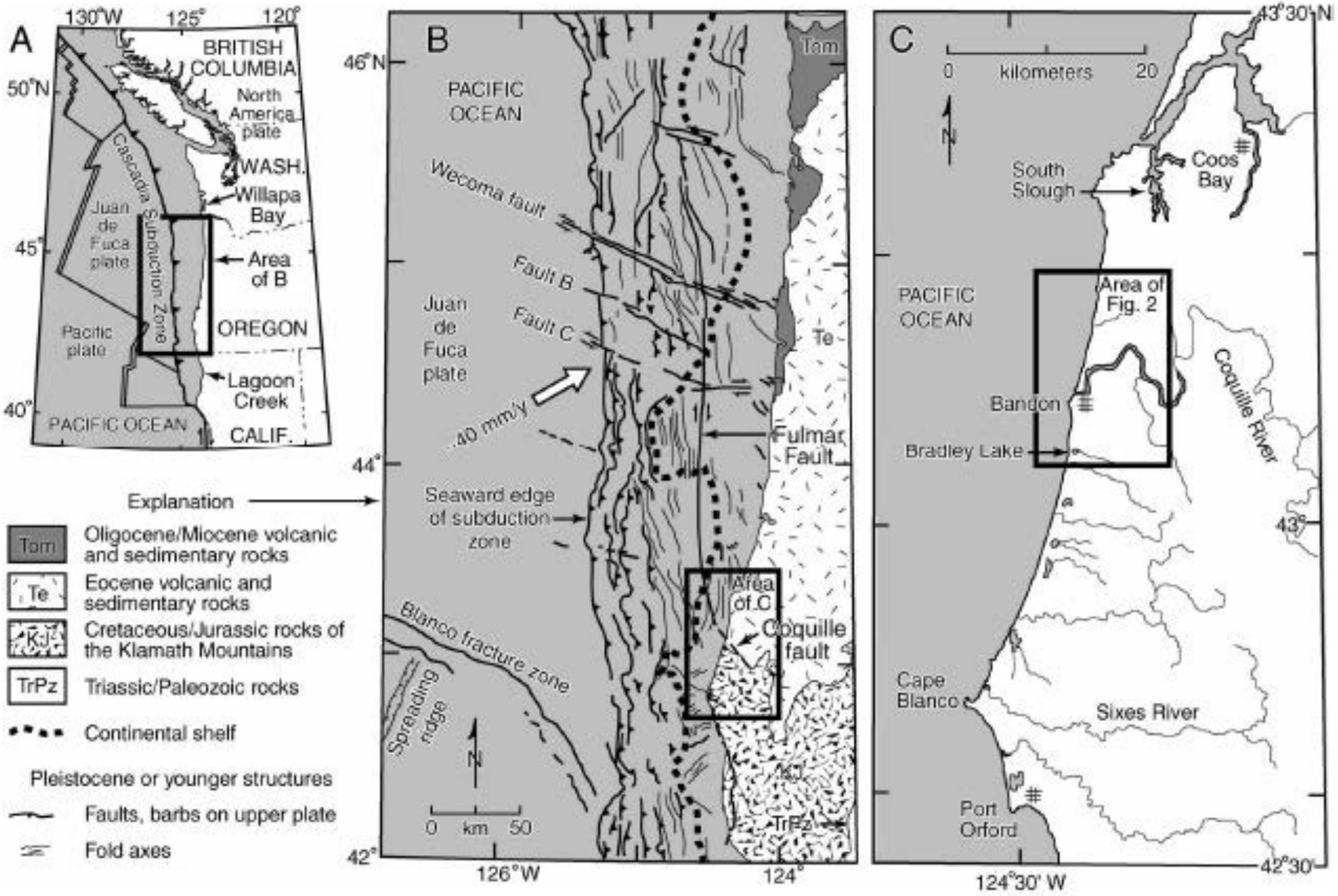

Figure 1. (A) Tectonic setting of Cascadia subduction zone. (B) Tectonic map of ocean floor and generalized geologic map of western Oregon. Offshore data from Snavely (1992) and Goldfinger et al. (1992); onshore data from Walker and MacLeod (1991). Juan de Fuca plate is obliquely subducting beneath North America plate at ~40 mm/yr. (C) Location map of Coquille River estuary in southwestern Oregon ~25 km south of South Slough estuary at Coos Bay.

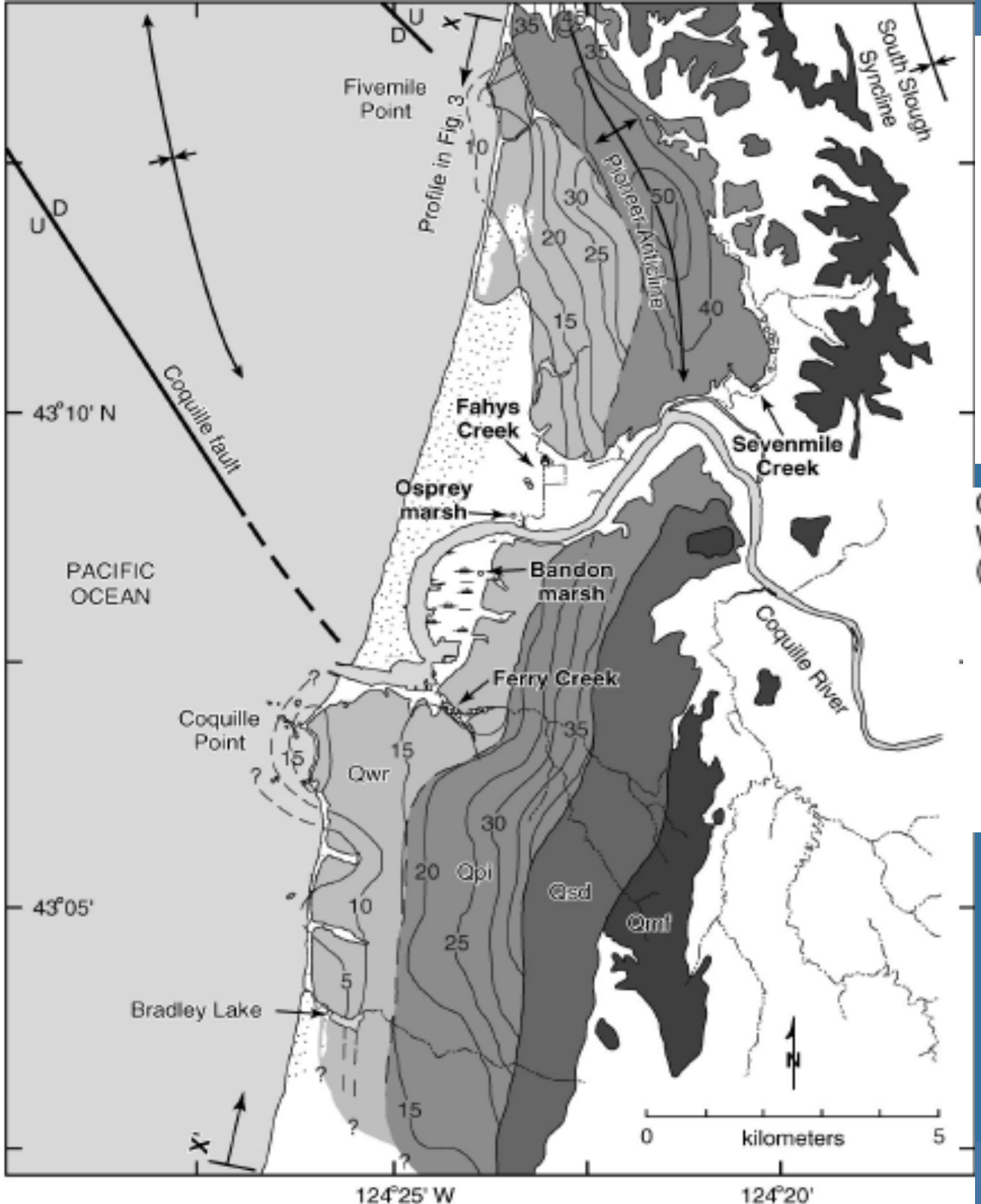

Late Pleistocene marine terraces

- Qwr — Whiskey Run marine terrace ~80,000 years old
- Qpi — Pioneer marine terrace ~105,000 years old
- Qsd — Seven Devils marine terrace ~125,000 years old
- Qmf — Metcalf marine terrace ≥200,000 years old

Contour lines (5-m interval) map the deformed Whiskey Run and Pioneer wave-cut platforms (after McInelly and Kelsey, 1990)

- Stratigraphic core sites shown in Figs. 5, 7, and 8
- Fold axes
- Fault, dashed where approximate


Whiskey run Terrace ~80,000 yr

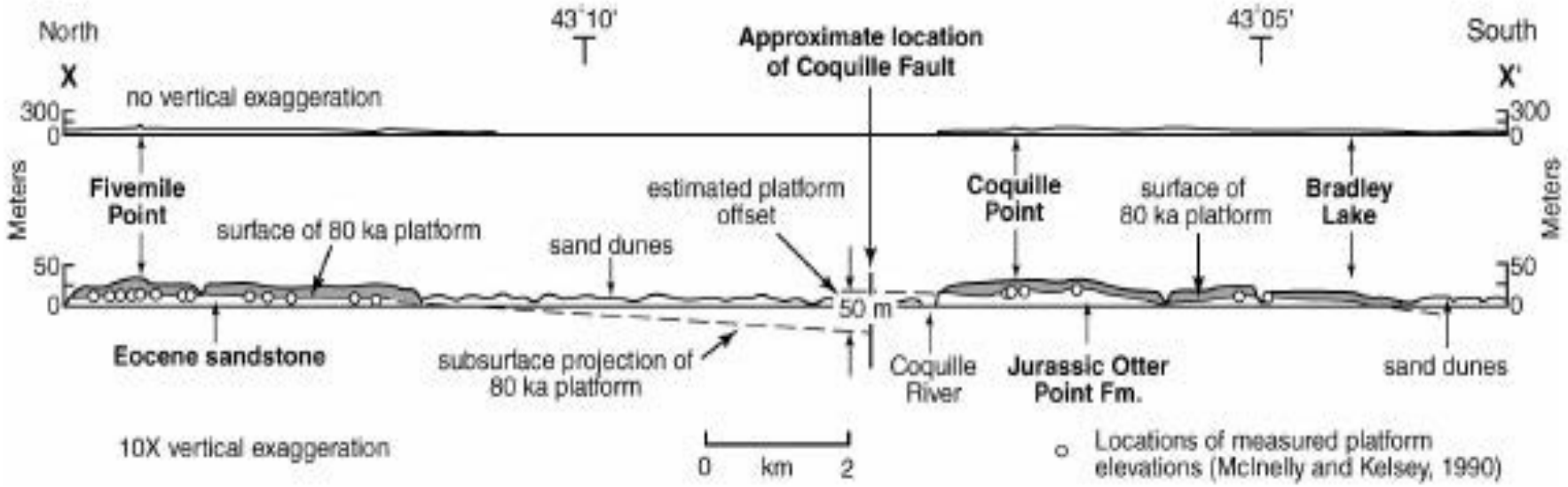

Figure 3. Coast-parallel profile (located on Fig. 2) showing variation in elevation of 80,000-yr-old Whisky Run wave-cut platform (McInelly and Kelsey, 1990). Southward-tilting platform near Fivemile Point is projected to inferred location of Coquille fault. Similarly, tilt of emergent platform at Coquille Point is projected northward to fault, where inferred platform offset is ~50 m. Offset may be less but is at least 18 m, highest elevation of platform at Coquille Point on up-thrown side of fault.

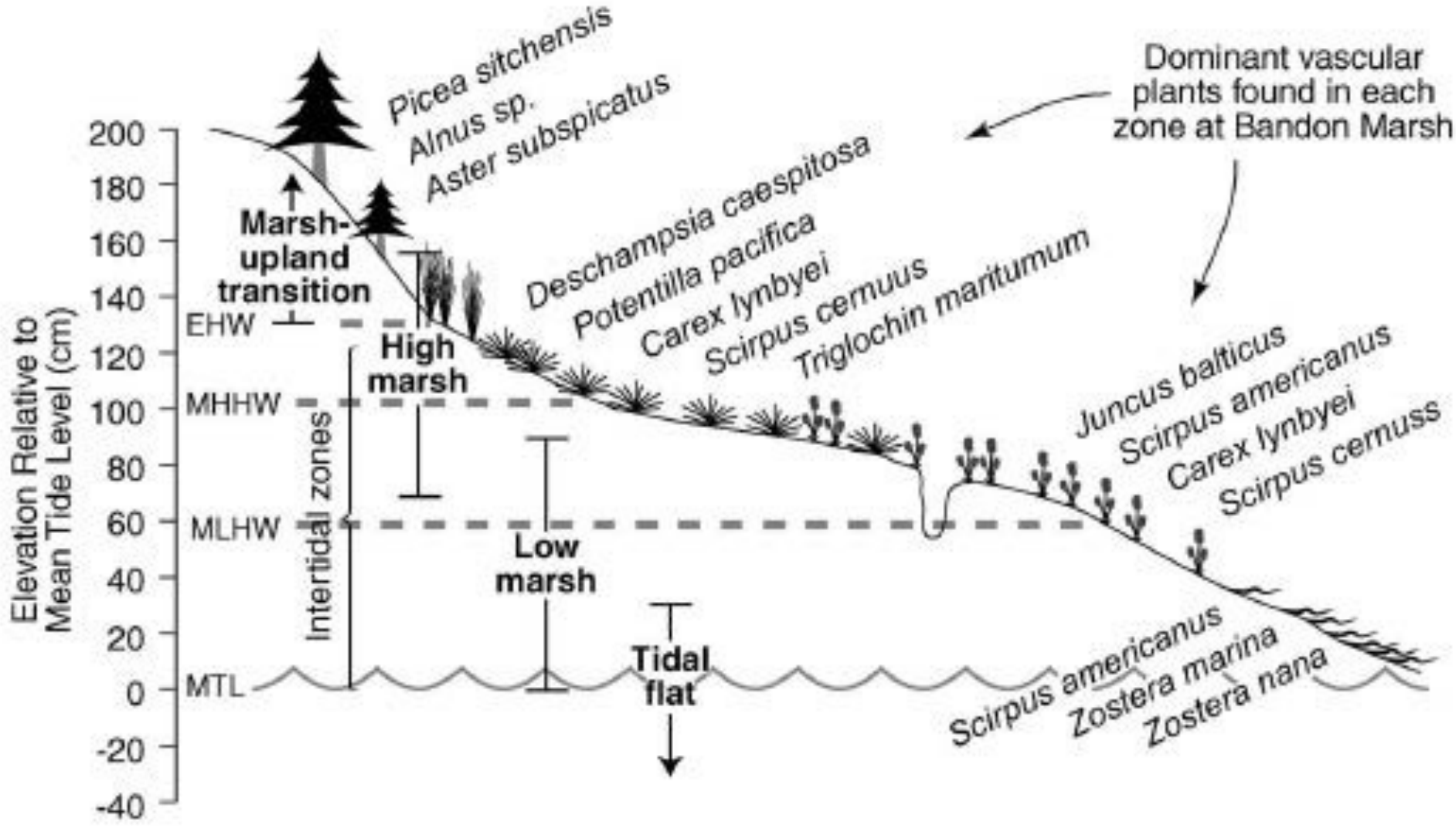

Figure 4. Elevation ranges for intertidal zones at Coquille River estuary based on distribution of vascular plants in Oregon tidal marshes (after Nelson and Kashima, 1993). Tidal data from National Ocean Service (1992): EHW, extreme high water; MHHW, mean higher high water; MLHW, mean lower high water; MLLW, mean lower low water; MTL, mean tide level. Intertidal zones overlap by 20–30 cm, reflecting vertical variation in zone boundaries (Nelson and Kashima, 1990) and include uncertainty in elevation of intertidal zones used to estimate paleo-mean tide level from fossil diatom assemblages (Table 3).

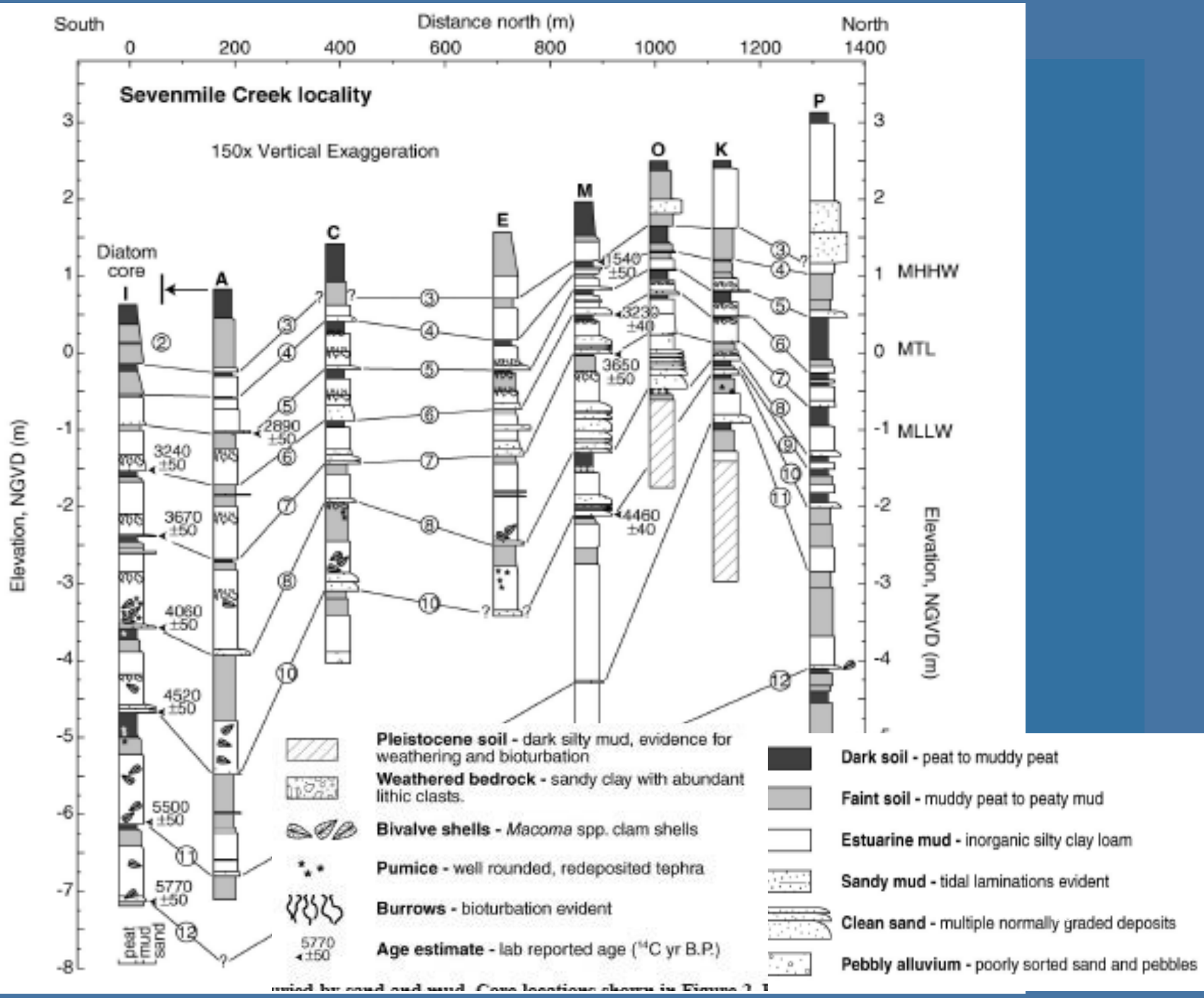

buried by sand and mud. Core locations shown in Figure 2-1

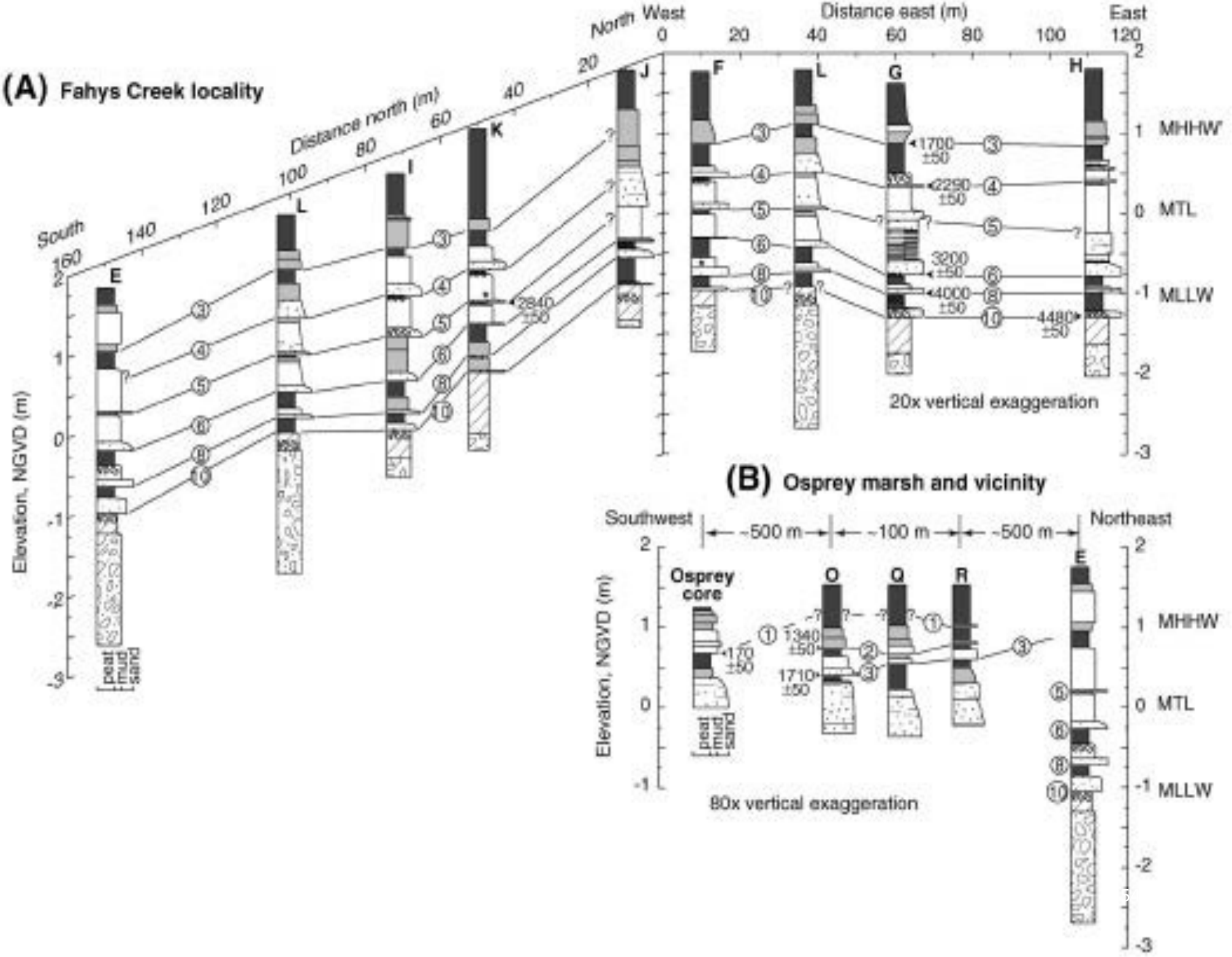

Figure 7. (A) Stratigraphy of Fahys Creek locality. Numbers indicate soils buried by sand and mud. Core locations shown in Figure 2.

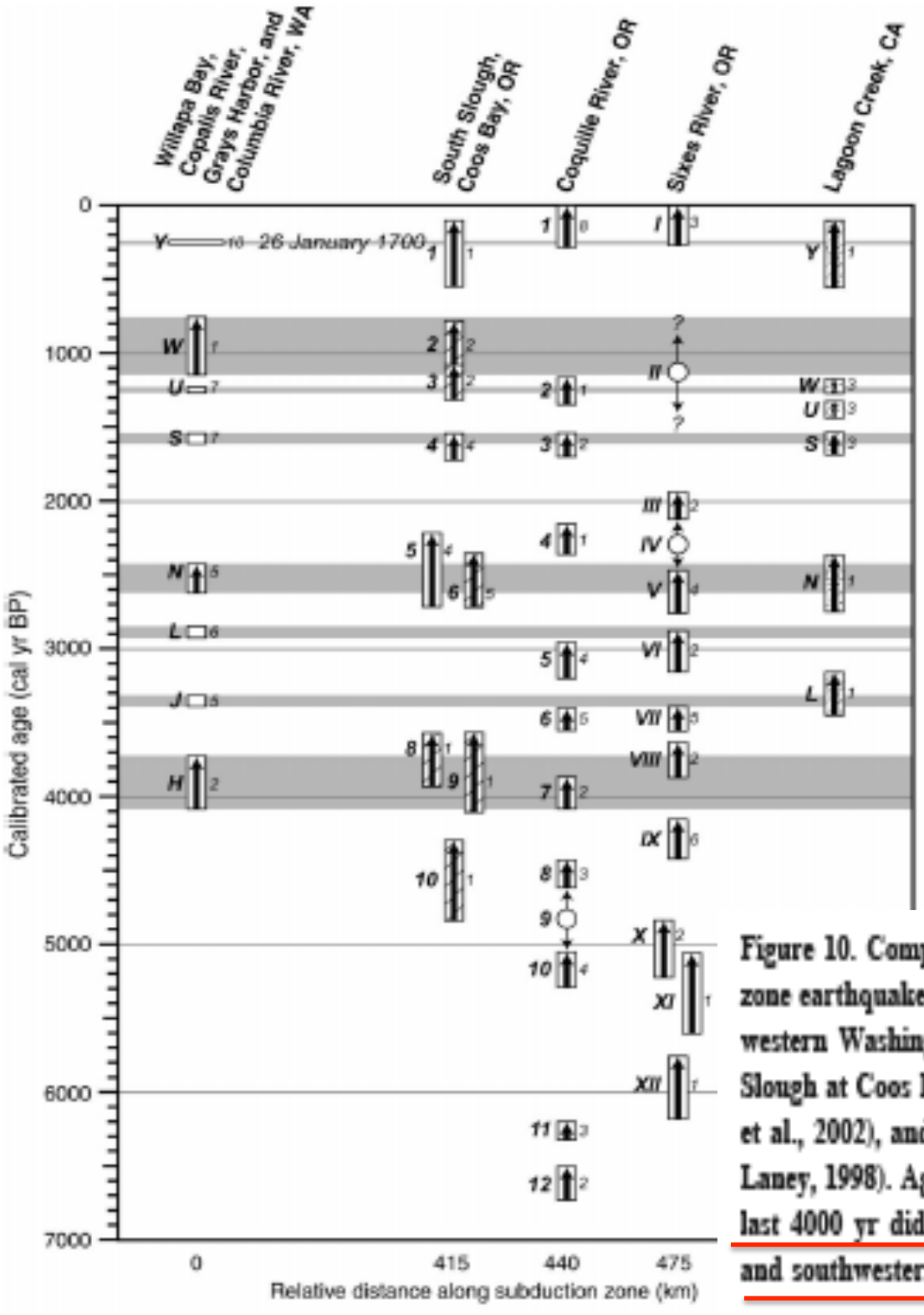

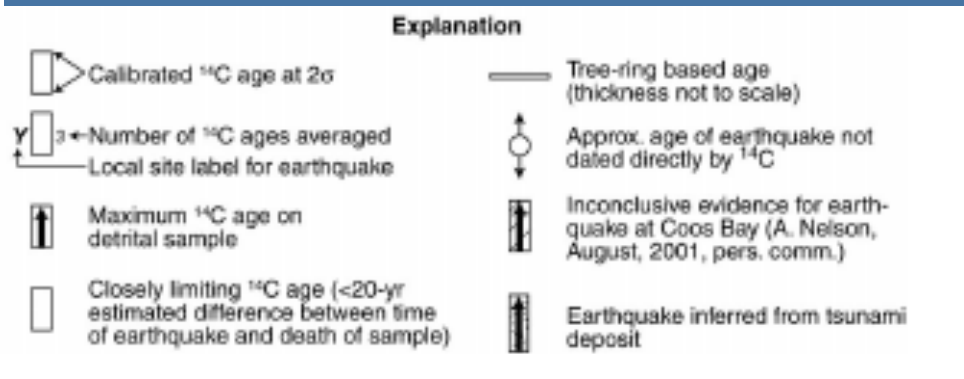

Figure 10. Comparison of calibrated radiocarbon age estimates for Cascadia subduction zone earthquakes recorded at Coquille estuary with earthquake age estimates from southwestern Washington (Atwater and Hemphill-Haley, 1997; Atwater, unpub. data), South Slough at Coos Bay (Nelson et al., 1996a, 1998; Nelson, unpub. data), Sixes River (Kelsey et al., 2002), and Lagoon Creek in northwestern California (Abramson, 1998; Garrison-Laney, 1998). Age comparisons suggest that at least two and possibly four earthquakes in last 4000 yr did not rupture entire subduction zone between southwestern Washington and southwestern Oregon.

Vertical Motions in Cascadia

Mitchell et al 1994

Cascadia Present Day Vertical Deformation

JGR 99 B6 pp 12,257-12,277.

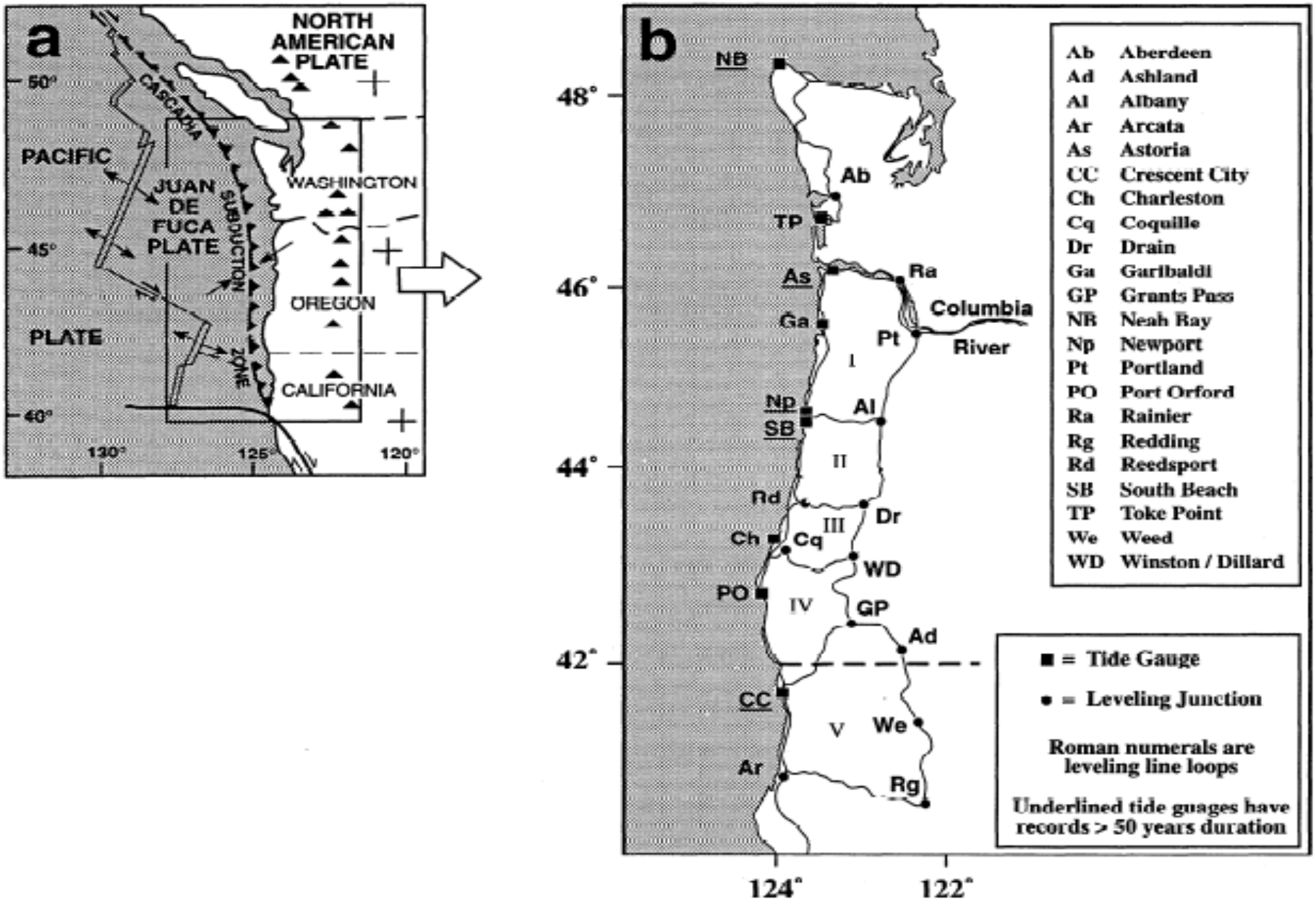

Figure 1. (a) Plate tectonic map of the Pacific Northwest. Arrows indicate direction of motion across major boundaries and triangles are volcanoes in the arc. Box outlines area covered by Figure 1b. (b) Index map of tide gauges and leveling lines used in this study. Dots are level line junctions; squares are tide gauges. Level lines form a network along the coast above the subduction zone, including north-south lines along the coast, and along the inland valleys east of the Coast Ranges, with numerous east-west connecting lines across the Coast Ranges. Roman numerals are level line loop numbers. Underlined tide gauge locations have records longer than 50 years.

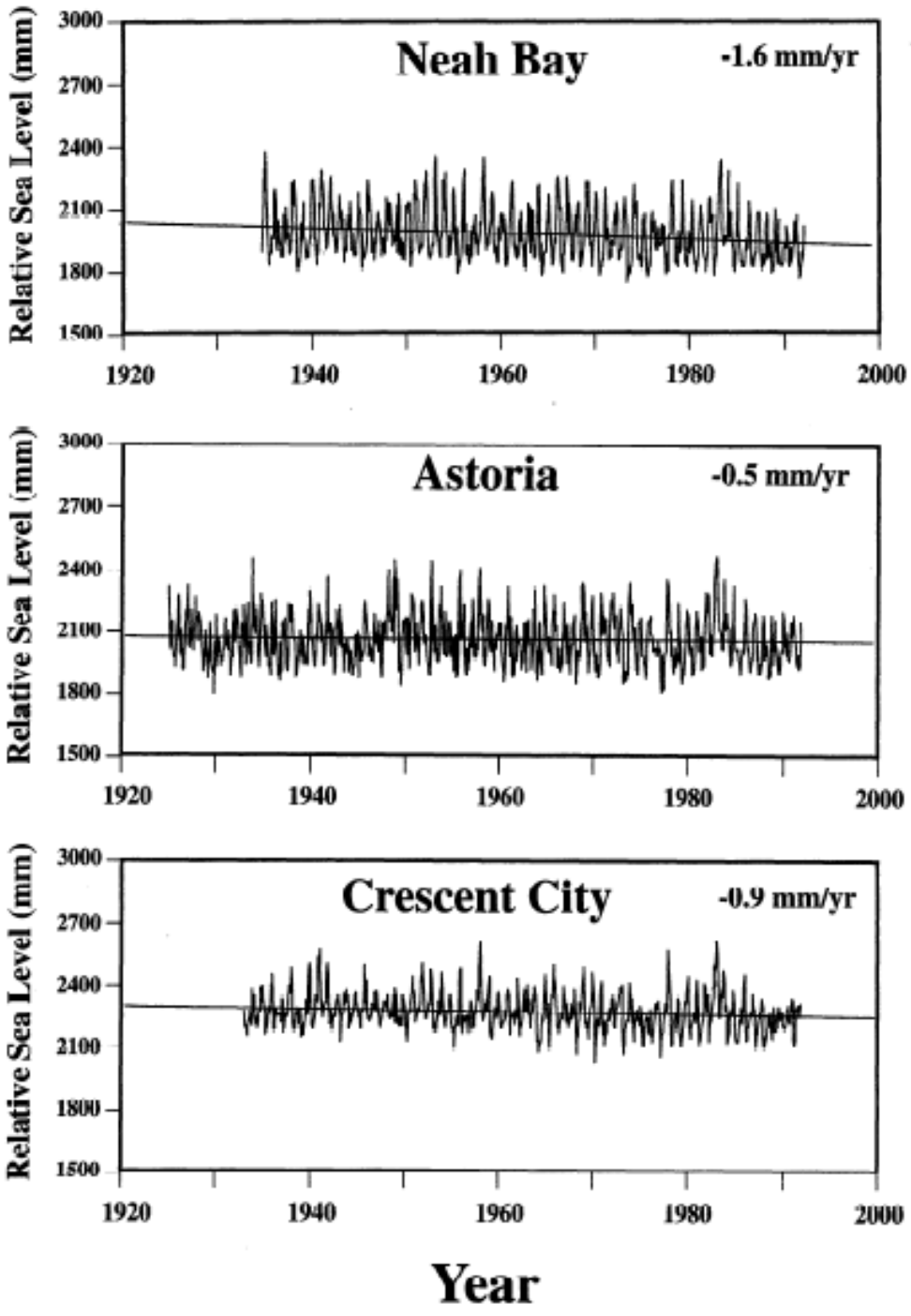

Figure 2. Records for relative sea level change for three stations with long-term records (> 50 years): (a) Neah Bay, (b) Astoria, and (c) Crescent City, with the best fit linear rate of relative sea level change noted for each. Points are monthly mean sea level; vertical datum for each station is arbitrary. The most obvious frequency is the seasonal cycle. Relative fall of sea level at all three stations indicates a dominance of uplift along this coast. Astoria rate is modified in subsequent figures, to correct for changes in Columbia River discharge.

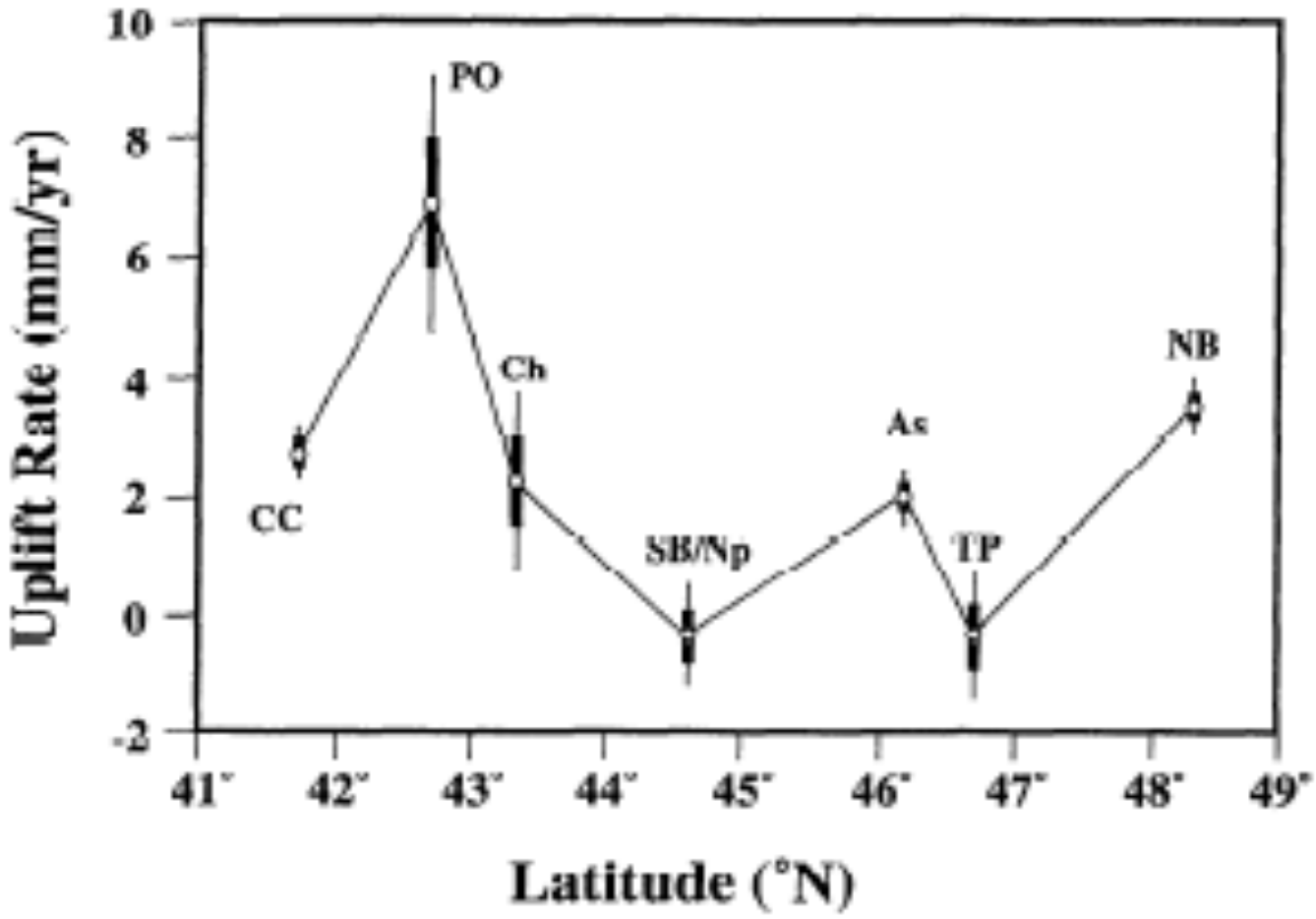

Figure 9. Profile of tectonic uplift rate inferred from relative sea level change along the Cascadia Margin. Stations are Neah Bay (NB), Toke Point (TP), Astoria (As), South Beach (SB), Charleston (Ch), Port Orford(PO), and Crescent City (CC). Each data point is mean uplift rate and includes 1.8 ± 0.1 mm/yr global sea level rise. Thick bars are 1 SE, as derived from the mean of the monthly average rates of change; thin bars enclose 2 SE. Note that the variation between adjacent stations is generally more than 2 SE. Data are summarized in Table 2.

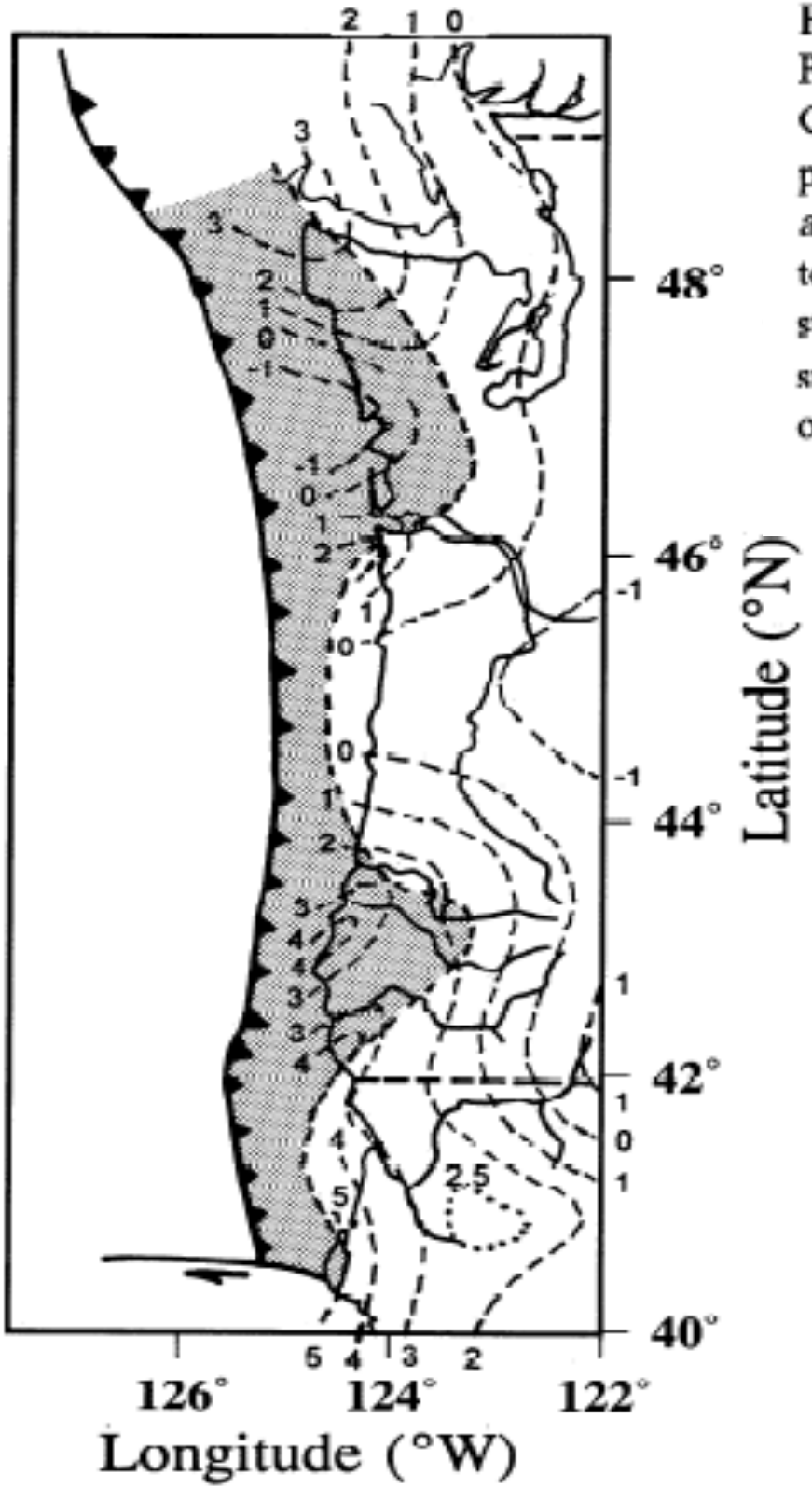

Figure 15. Contour map of present-day uplift rates in the Pacific Northwest, west of the Cascade Range and south of Canada. Contours are generated from tidal records and leveling profiles, with much of Washington state recontoured from *Ando and Balazs* [1979] and *Holdahl et al.* [1989], as discussed in the text. The stippled area is an interpretation of the region of elastic strin accumulation, assuming that the most rapid uplift at the surface approximately overlies the downdip edge of that portion of the subduction interface [*Savage*, 1983].

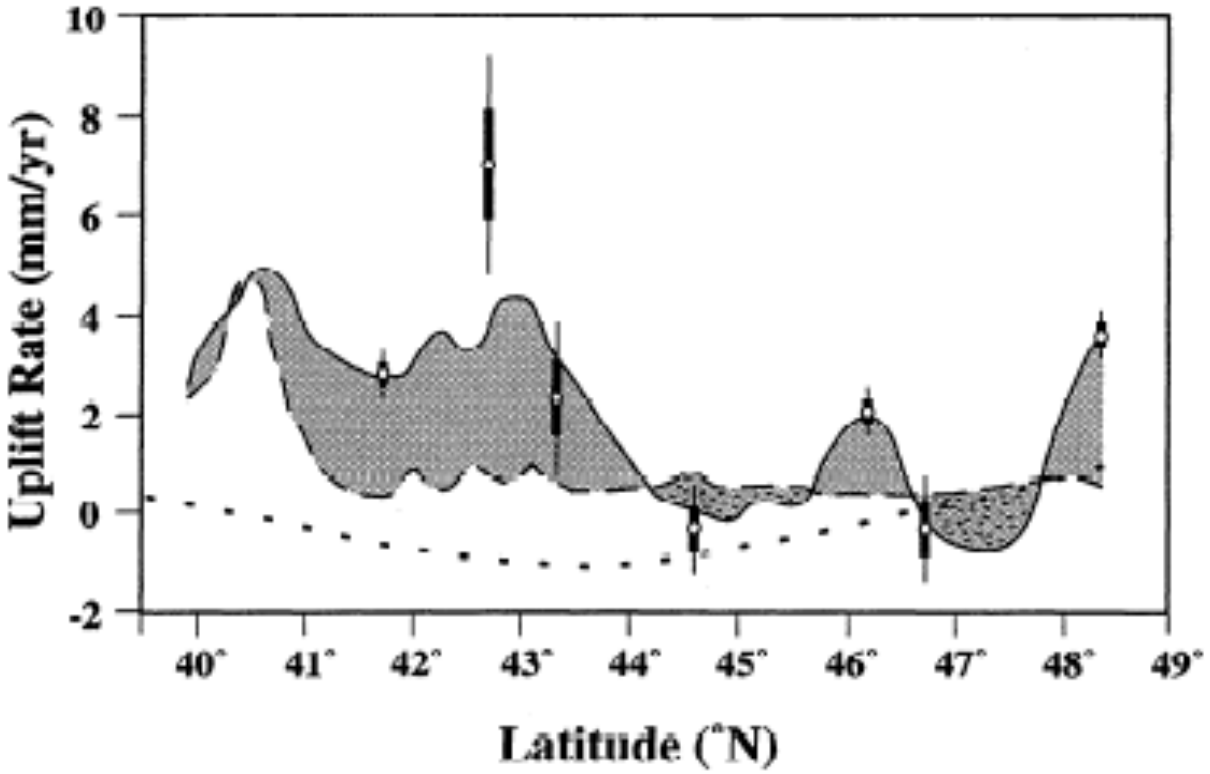

Figure 16. Comparison of the coastal uplift rate profile from releveling (dark solid line), tidal data (points with error bars), and marine terrace studies (dashed) by *Merritts and Bull* [1989] for 40-41°N, *Kelsey et al.* [this issue] for 42-45°N, and *West and McCrumb* [1988], elsewhere. Uplift rates from various authors may not be strictly comparable, but the difference between rates on present-day versus permanent time scales is still obvious. The dotted line is an approximate cross section from the map of estimated North American postglacial rebound by *Peltier* [1986]. Stippled regions are inferred to represent elastic strain accumulation; note that some areas will go up (coarse stippling) and others will go down (fine stippling), when this strain is released coseismically.

Tectonics of the Neogene Cascadia forearc basin: Investigation of a deformed late Miocene unconformity

McNeil et al 2000

GSA Bulletin pp. 1209-1224.

(What do we see offshore?)

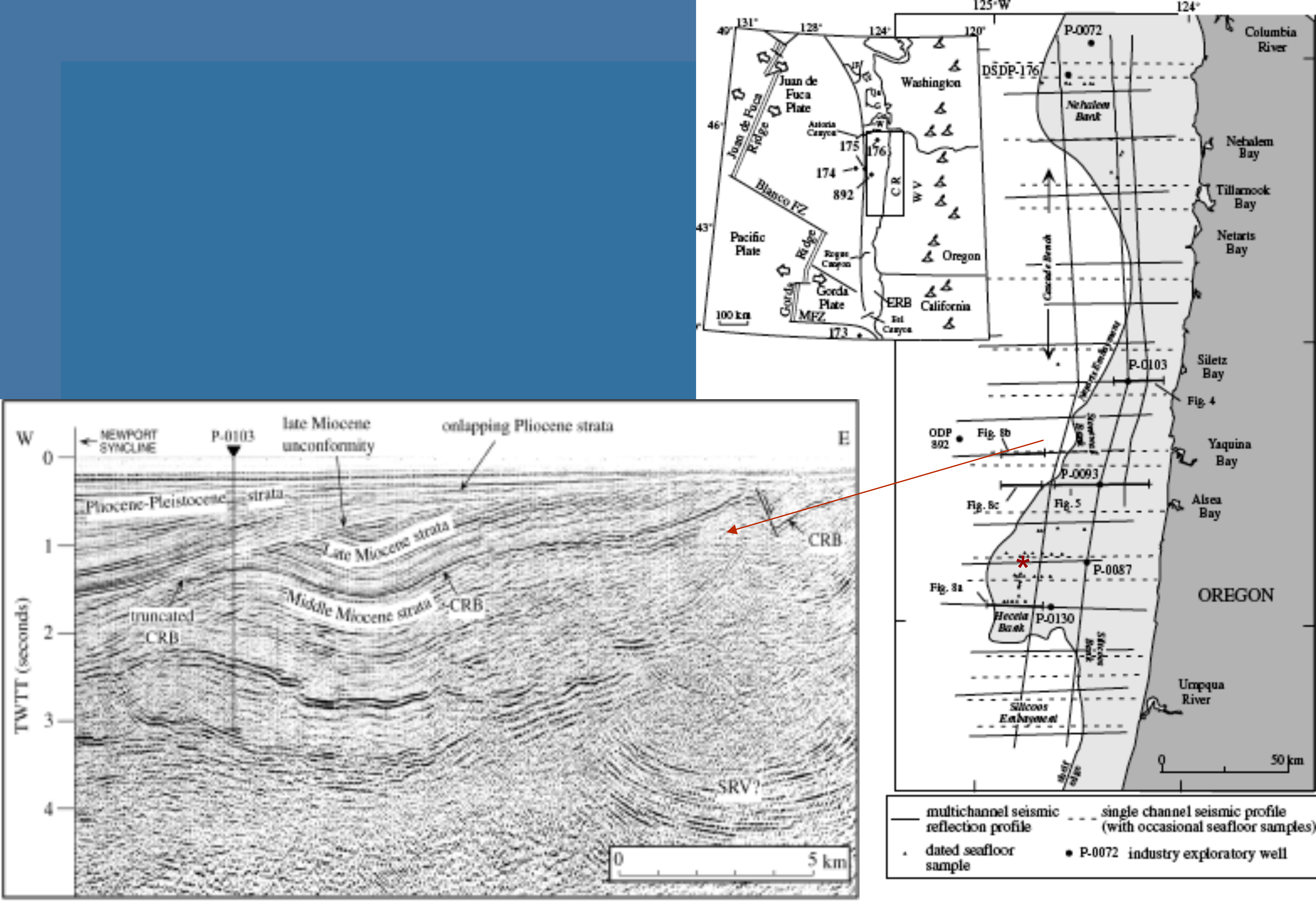
W
E
NEWPORT SYNCLINE
P-0103
late Miocene unconformity
onlapping Pliocene strata
Pliocene-Pleistocene strata
Late Miocene strata
Middle Miocene strata
truncated CRB
CRB
SRV?
TWTT (seconds)
0
1
2
3
4
0
5 km
125°W
124°
46°N
45°
44°
131°
128°
124°
120°
49°
46°
43°
Juan de Fuca Plate
Juan de Fuca Ridge
Blanco FZ
Gorda Ridge
Pacific Plate
Gorda Plate
MFZ
Astoria Canyon
Rogue Canyon
Eel Canyon
175
176
174
892
173
CR
WV
ERB
Washington
Oregon
California
100 km
P-0072
DSDP-176
Nehalem Bank
Columbia River
Nehalem Bay
Tillamook Bay
Netarts Bay
Cascadia Bench
Siletz Bay
P-0103
Fig. 4
ODP 892
Fig. 8b
Yaquina Bay
P-0093
Alsea Bay
Fig. 8c
Fig. 5
P-0087
Fig. 8a
Heceta Bank
P-0130
OREGON
Siltcoos Embayment
Umpqua River
0
50 km
multichannel seismic reflection profile
single channel seismic profile (with occasional seafloor samples)
dated seafloor sample
P-0072 industry exploratory well

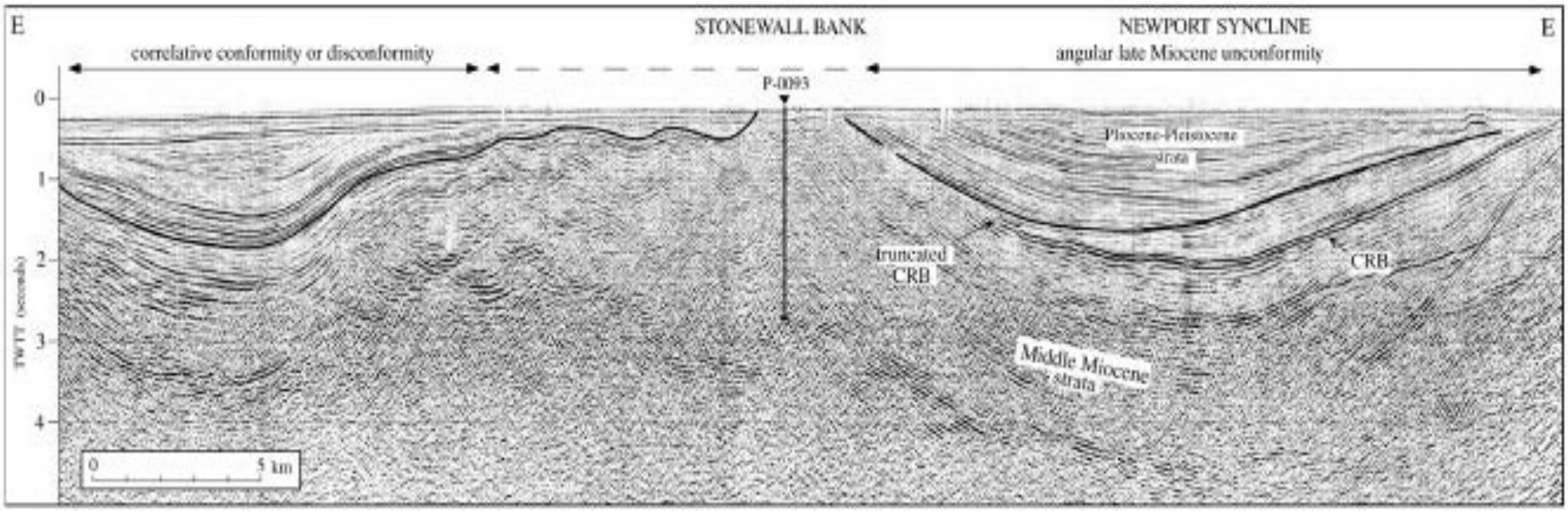

Figure 5. East-west multichannel seismic reflection profile across the continental shelf at Stonewall Bank west of Alsea Bay (Fig. 1). The late Miocene unconformity (bold black line) is angular landward of Stonewall Bank anticline, slightly angular just west of the bank where small wavelength folds are truncated, and conformable or disconformable seaward of these folds. This profile typifies the character of the unconformity from east to west. Note that the unconformity truncates the late Miocene Columbia River Basalt flow (CRB) just east of well P-0093. Pliocene sediments onlap landward at a very low angle at the eastern end of the profile and are parallel to the unconformity elsewhere, indicating little relief on the unconformity at the time of erosion. After Yeats et al. (1998).

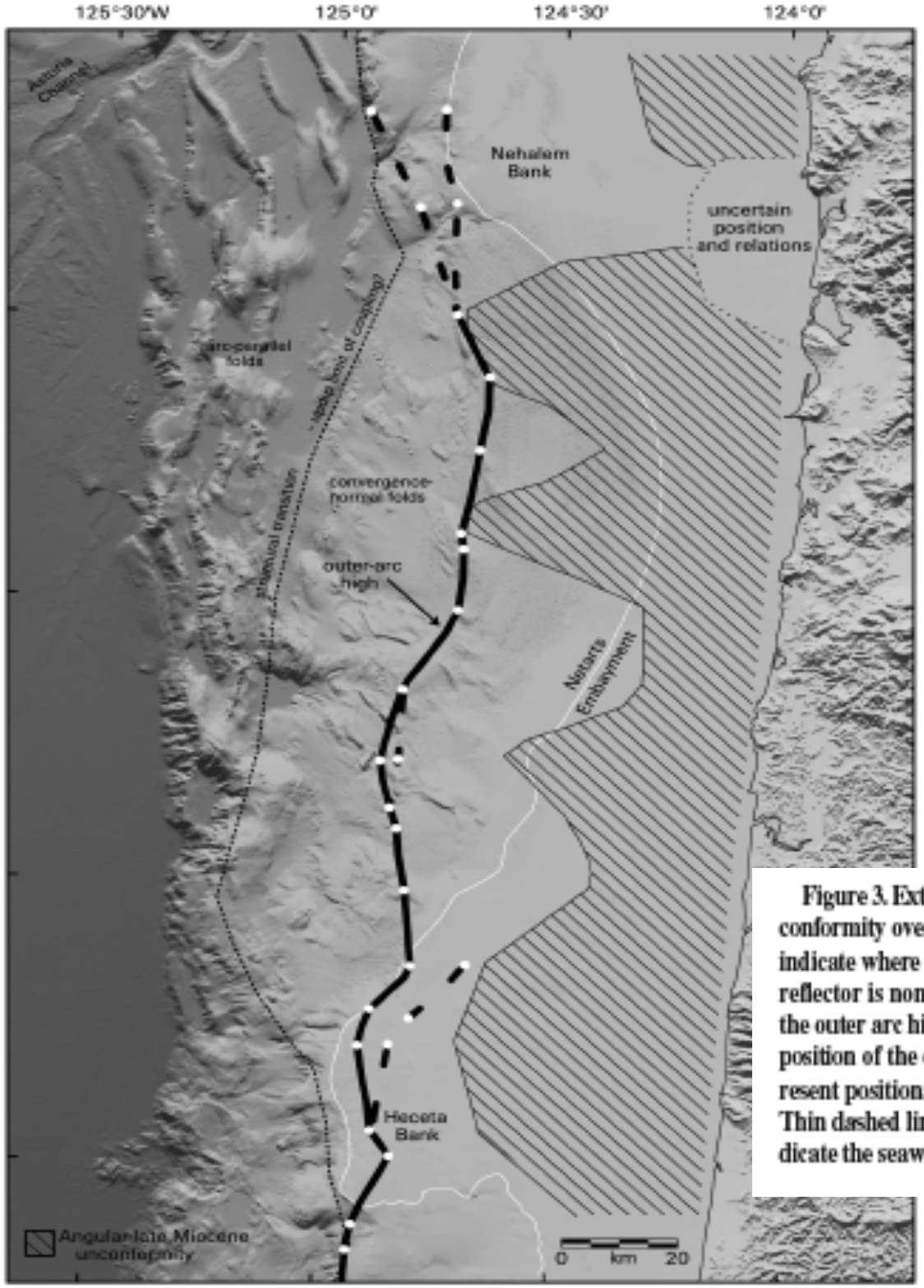

Figure 3. Extent of the late Miocene unconformity and correlative seaward conformity or disconformity overlying shaded relief bathymetry base map of the Oregon margin. Diagonal lines indicate where the unconformity is clearly an angular unconformity. Elsewhere, the correlative reflector is nonangular or partially angular but can still be traced as a continuous reflector to the outer arc high. White line represents present-day shelf break. Thick black line indicates the position of the outer arc high marking the seaward extent of the forearc basin, white dots represent positions on seismic profiles, dashed lines indicate alternative outer arc high positions. Thin dashed line represents a topographic break and change in fold orientation which may indicate the seaward extent of interplate coupling (Goldfinger et al., 1996b).

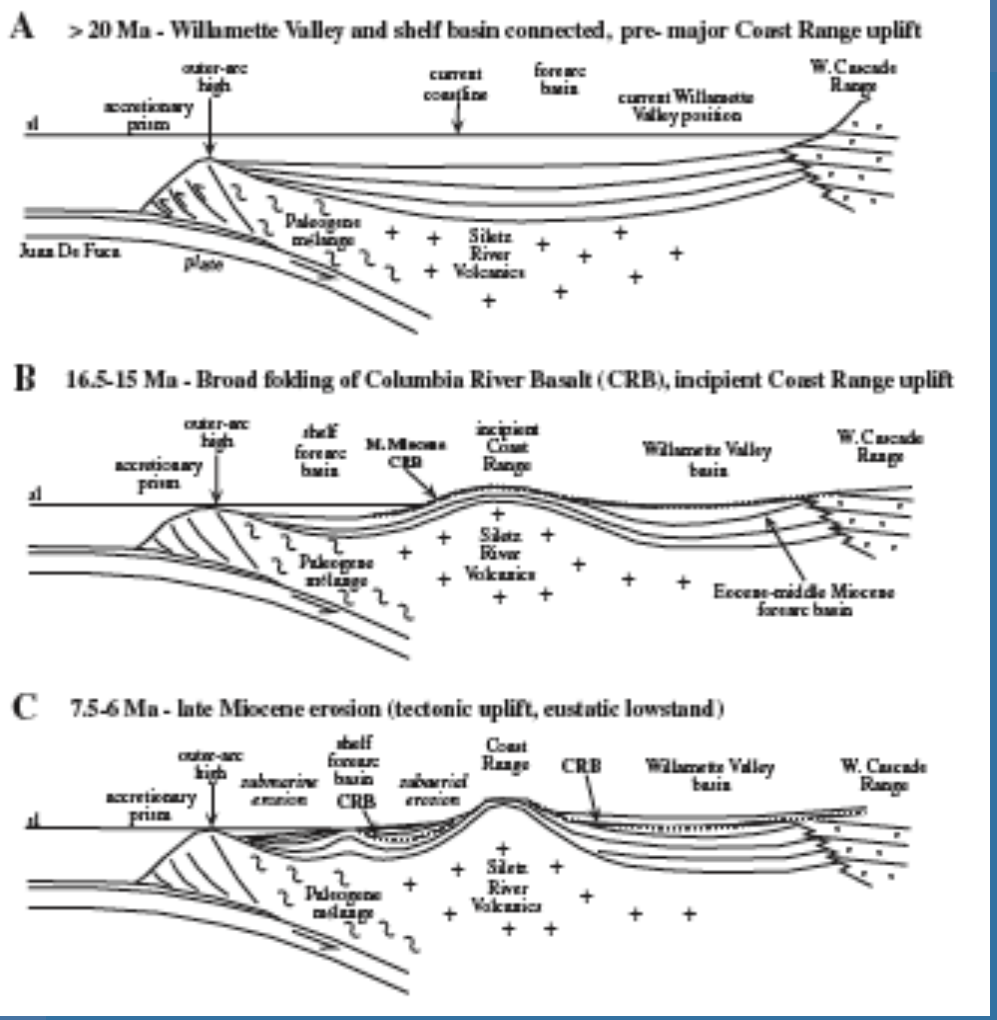

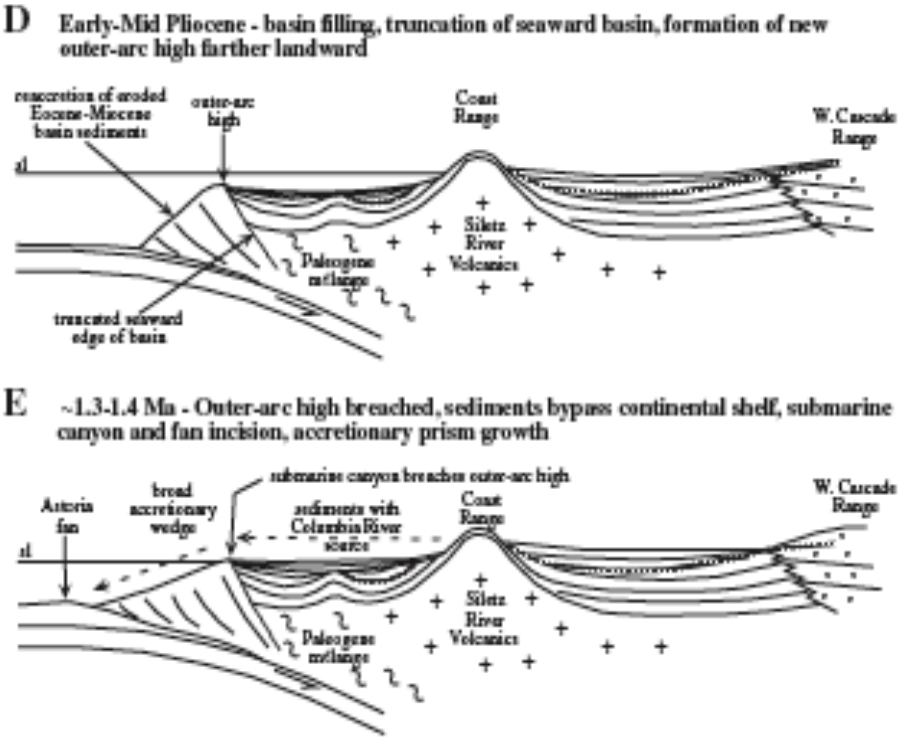

Figure 9. Neogene tectonic history of the central Cascadia forearc depicted by time slice cross sections of the central Oregon forearc from the Cascades to the deformation front. Stratigraphy and topographic features are generalized for the central Oregon forearc. (A) The Willamette Valley and shelf basins connected prior to major uplift of the Coast Ranges (with local highlands existing). (B) Columbia River Basalt emplacement and incipient Coast Range uplift. (C) Erosion of the late Miocene unconformity. (D) Pliocene basin filling and truncation of the seaward edge of the offshore basin. (E) Shelf basin filling and submarine fan formation in the Pleistocene.

Slow-slip phenomena in Cascadia

Gomberg et al 2010

GSA Bulletin B30287

Figure 1. Schematic tectonic map of Cascadia. Major provinces (shaded areas and italicized labels) are distinguished by the dominant deformation style and rates, stress fields that drive the deformation, and geologic histories and structures. Arrows straddling major plate boundaries indicate relative plate motions, and other solid curves schematically show trends and types of crustal faults within the North American plate. Triangles denote volcanoes. Figure is modified from Wells and Simpson (2001).

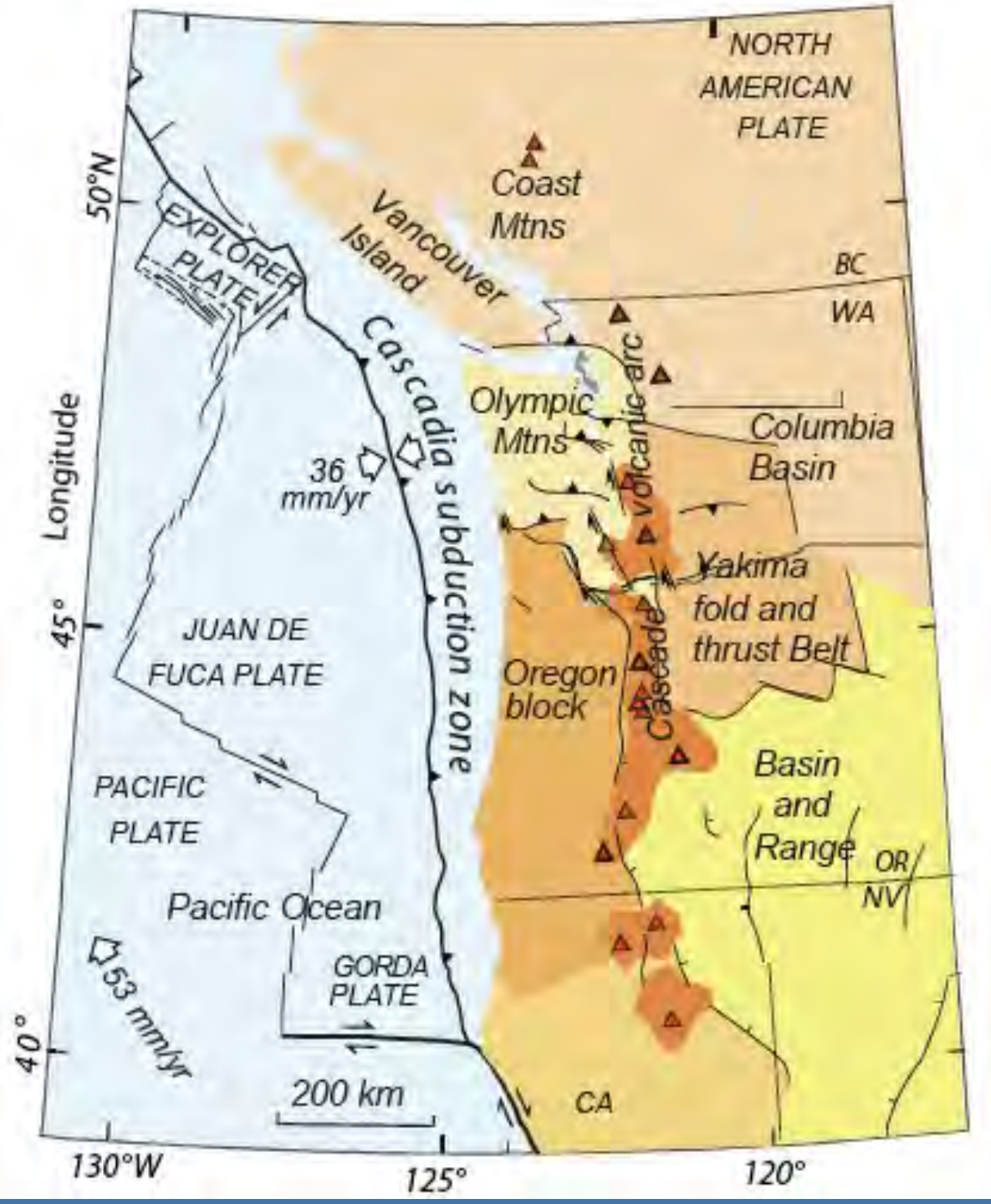

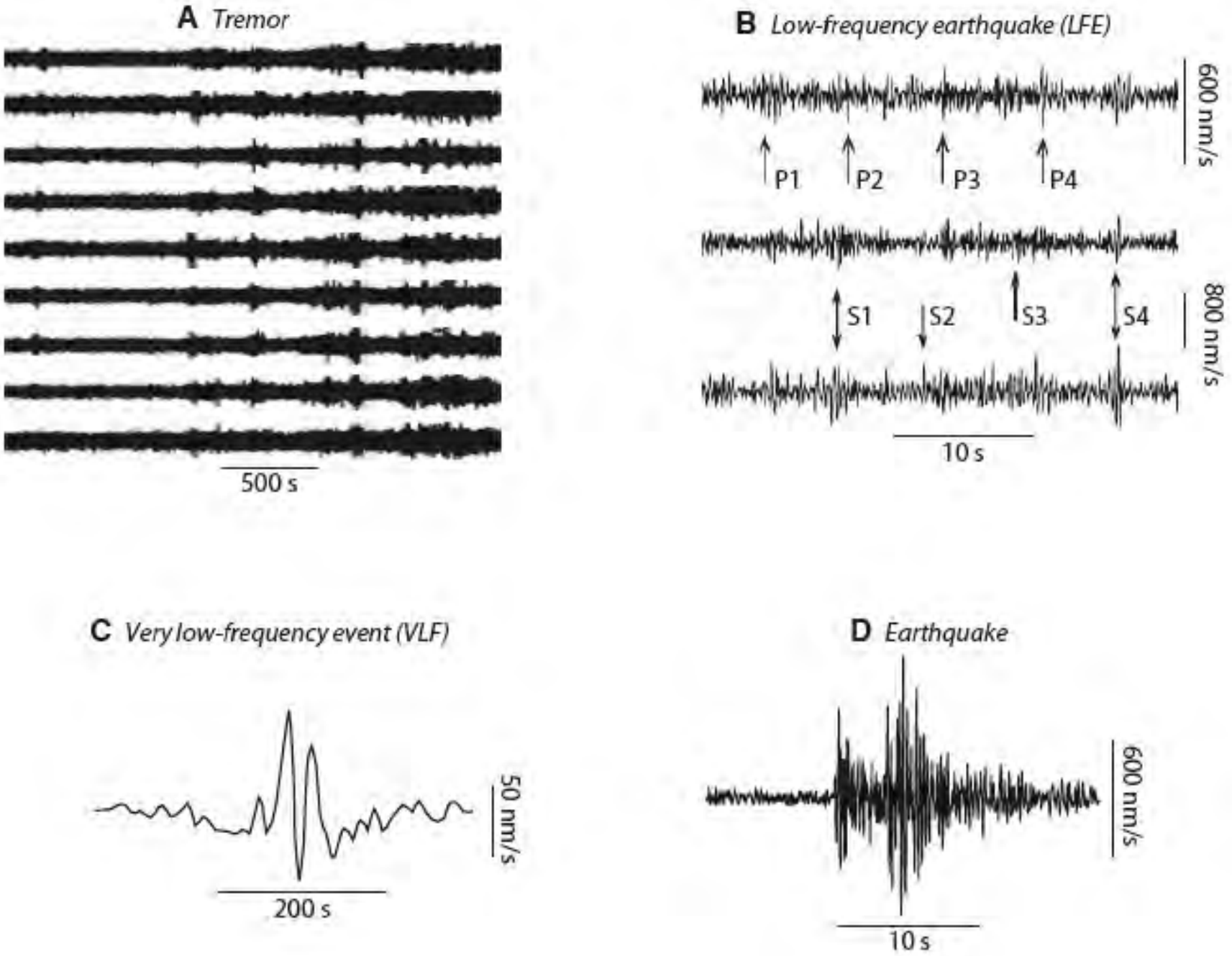
A Tremor
500 s
B Low-frequency earthquake (LFE)
600 nm/s
P1
P2
P3
P4
S1
S2
S3
S4
800 nm/s
10 s
C Very low-frequency event (VLF)
50 nm/s
200 s
D Earthquake
600 nm/s
10 s

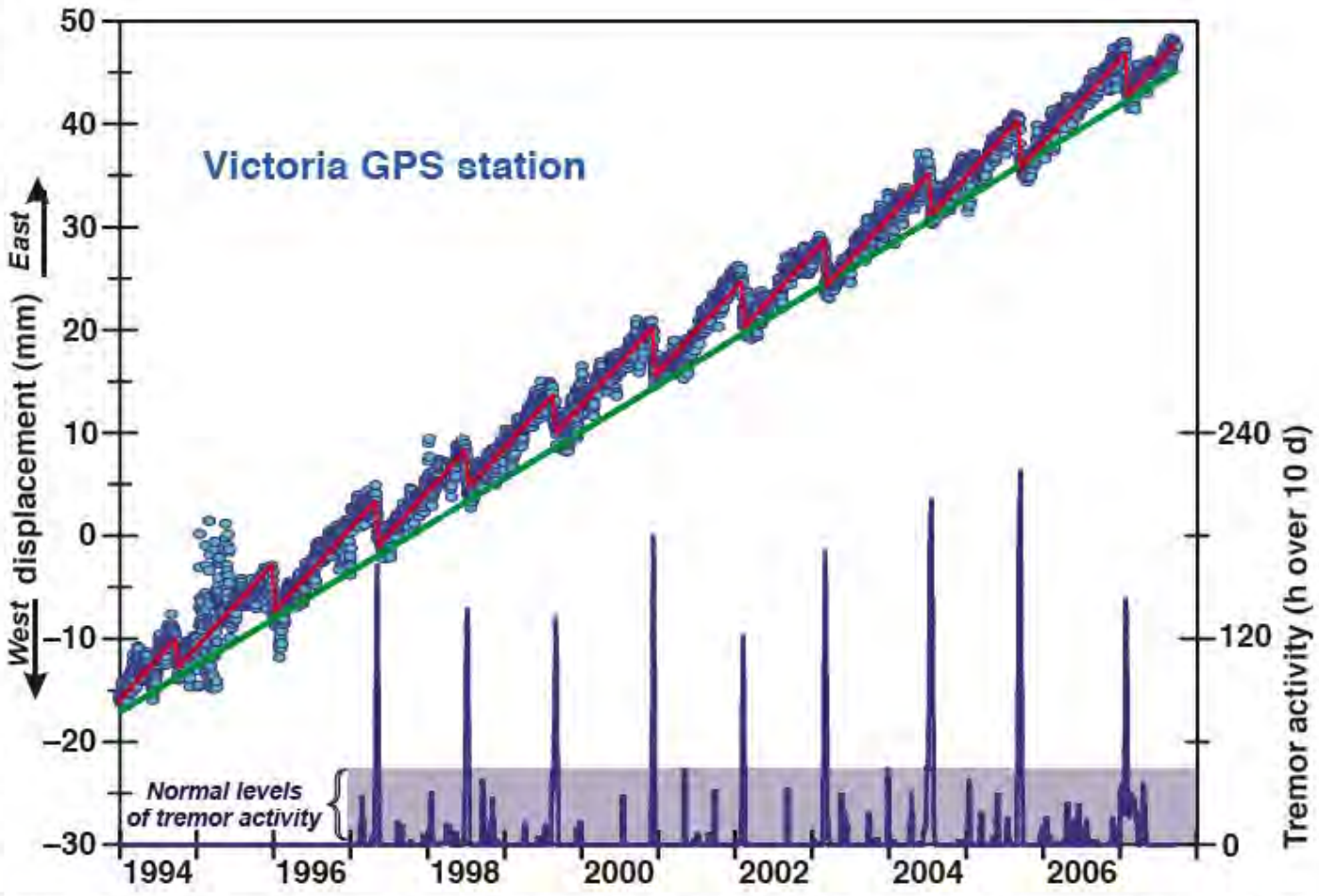

Figure 4. Iconic display of episodic tremor and slip (ETS) in Cascadia showing the synchronous occurrence of slow slip and vigorous tremor activity. Daily changes in measured east-west displacements of the global positioning system (GPS) station at Victoria, British Columbia, relative to stable North America (blue circles) show that the site moves eastward on average at ~5 mm/yr (green line). It does so in a sawtooth fashion by moving eastward more rapidly than the average for 15 mo and then westward ~4 mm over a period of 2 wk (red line). These transient reversals are caused by slow slip on the deeper plate interface. Tremor activity occurs throughout the year generally for less than a few hours per day, except during slow-slip events, when activity is seen to increase by more than an order of magnitude. Only analog seismic data exist prior to 1996, and the same pattern is apparent in these but is not easily quantified. Figure is updated from Rogers and Dragert (2003).

Gomberg et al 2010

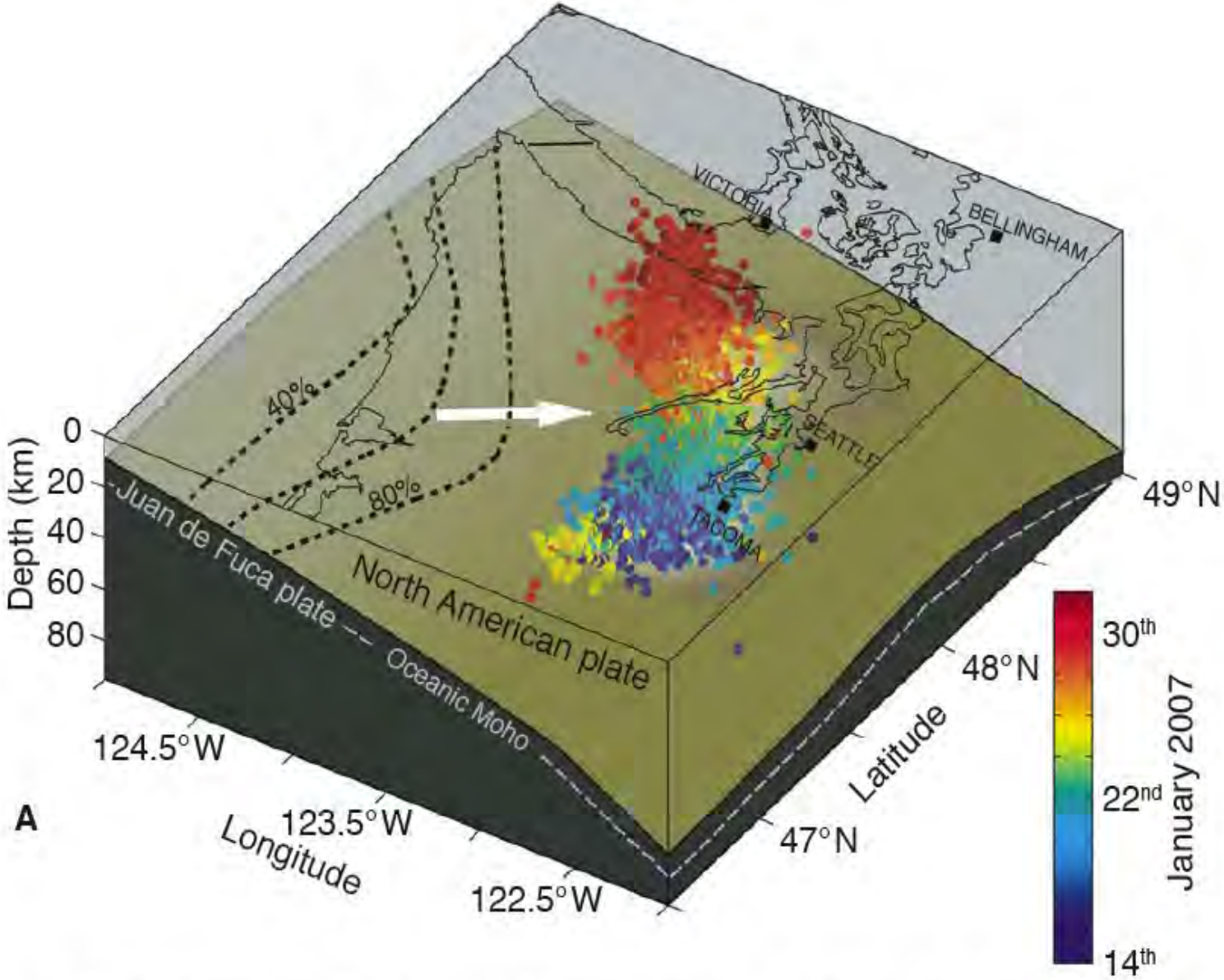

Figure 3 (*on this and following page*). **Illustration of northern Cascadia and 2007 episodic tremor and slip (ETS) event. (A) The oceanic Juan de Fuca plate sinks or subducts beneath the continental North America plate with an ~4 cm/yr convergence direction, roughly perpendicular to the coast (white arrow). The plates are coupled at part of their interface (khaki-colored surface) such that relative motion is inhibited or "locked" to varying degree. The location and mechanism by which the locking changes to a freely slipping interface are uncertain. Here, we show one model in which the fraction of relative plate motion is portrayed as continuous aseismic slip that increases downdip from 40% to 80% (dashed contours) (McCaffrey et al., 2007). Inland of the locked zone, tremor epicenters projected onto the plate interface (circles) overlie the area that experienced slow slip (gray area on plate interface) during the last two weeks of January 2007. Color shading of tremor epicenters shows its temporal migration. Figure is from Forsyth et al. (2009).**

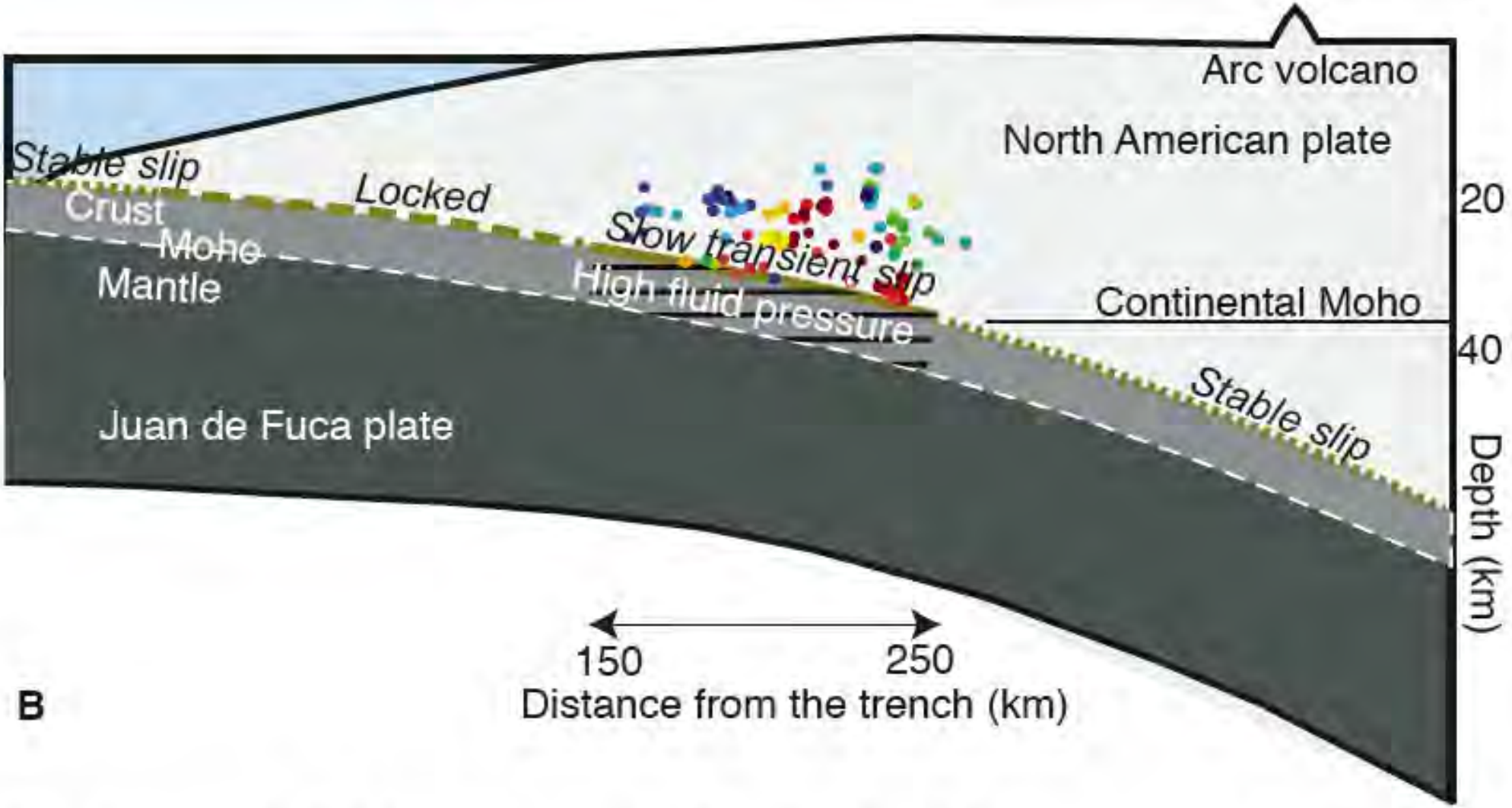

Figure 3 (*continued*). (B) Schematic cross section of the Cascadia subduction zone modified from Audet et al. (2009, 2010) and Kao et al. (2009). The various slip modes believed to occur along the plate interface are noted (khaki lines), and the corresponding observed phenomena indicative of each are listed below. The zone of high fluid pressure is inferred from seismic images and corresponds to the E-zone, the top of which has been inferred recently to be the plate interface where aseismic slow slip occurs. Tremor source location estimates concentrate at and above the interface (see text), albeit with large uncertainties.

New aeromagnetic data reveal large strike-slip (?) faults in northern Willamette Valley, Oregon

Blakely et al 2000
GSA Bulletin pp. 1225-1233

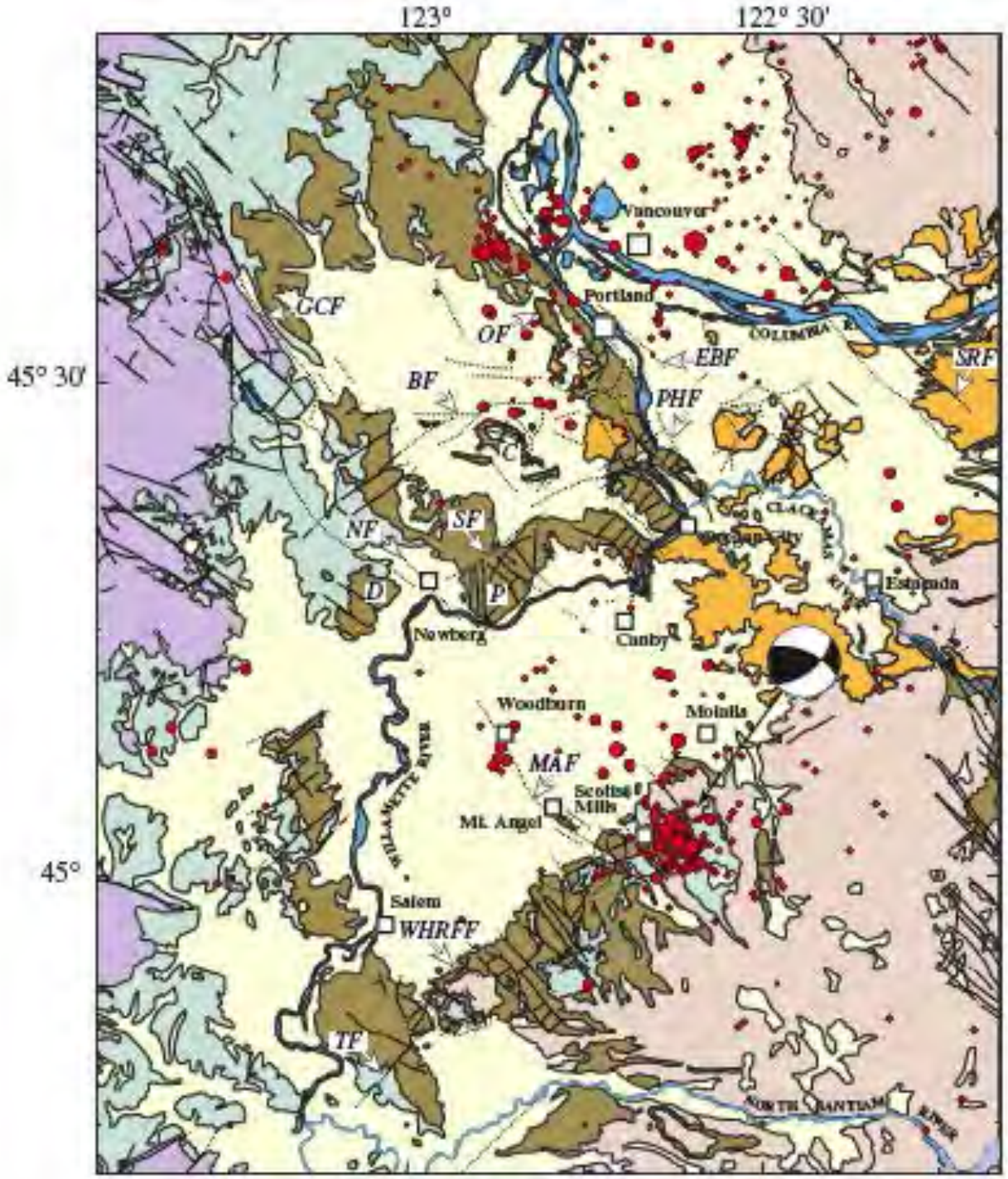

Miocene and younger deposits
Boring Lava
Columbia River basalt
Eocene-Paleocene sedimentary rocks
Volcanic rocks of the Western Cascades
Eocene oceanic basement

Fault
Anticline
Homocline

Earthquake Magnitude
0–1
1–2
2–3
3–4
5–6

0 25 km

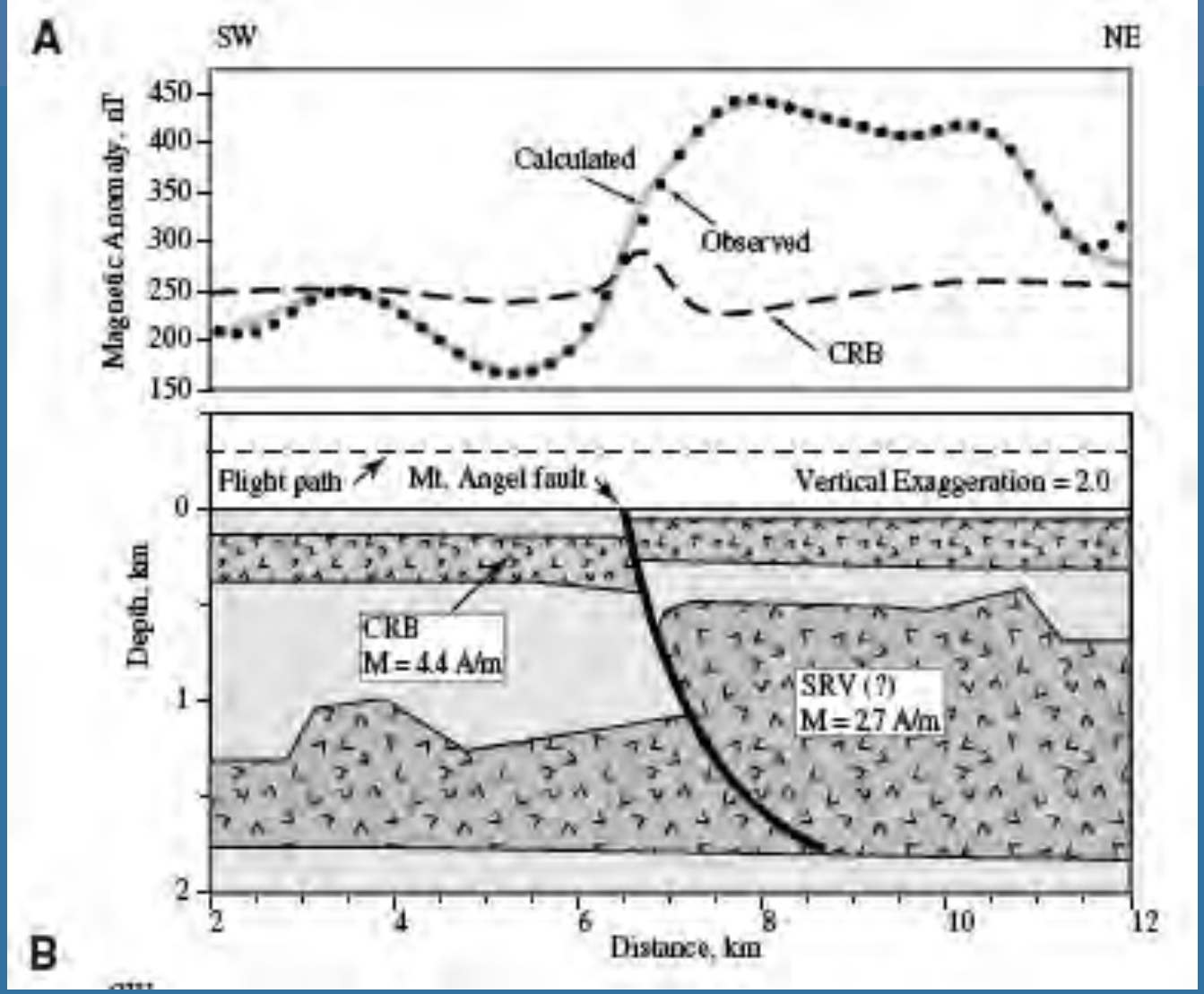
A
SW
NE
Magnetic Anomaly, nT
450
400
350
300
250
200
150
Calculated
Observed
CRB
Flight path
Mt. Angel fault
Vertical Exaggeration = 2.0
Depth, km
0
1
2
CRB
M = 4.4 A/m
SRV (?)
M = 2.7 A/m
2
4
6
8
10
12
Distance, km
B

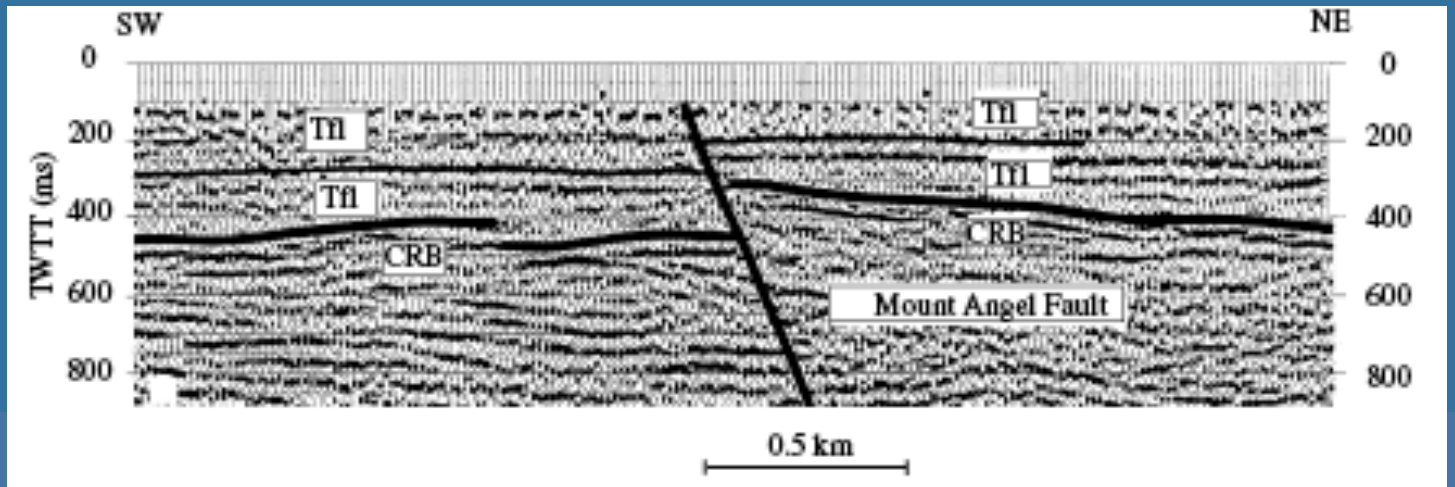
SW
NE
TWTT (ms)
0
200
400
600
800
Tfl
Tfl
Tfl
Tfl
CRB
CRB
Mount Angel Fault
0.5 km

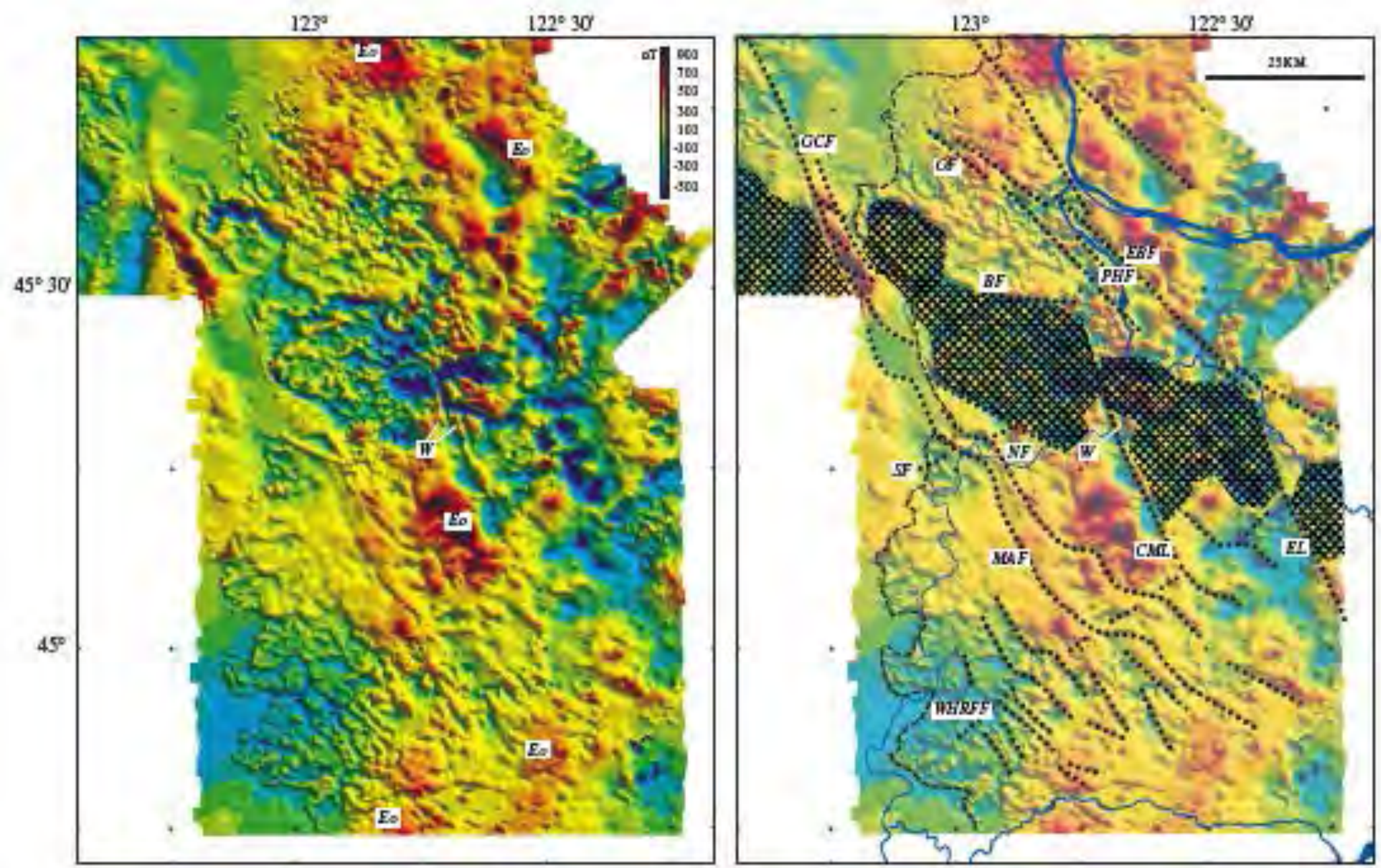

Figure 2. (A) Aeromagnetic anomalies of the northern Willamette Valley. Color scale represents intensity of crustal magnetic field, expressed in nanoteslas (nT). Eo—high-amplitude anomalies suspected of being caused by Eocene oceanic basalt basement. (B) Interpretation of aeromagnetic anomalies. Dotted lines indicate magnetic lineaments. Dashed line is western extent of Columbia River basalt flows. Cross-hachured areas are magnetic lows discussed in text. CML—Canby-Molalla lineament; EL—Estacada lineament; W—anomaly across Willamette River dextrally offset along Canby-Molalla lineament. See Figure 1 caption for other abbreviations.

Earthquake Hazard Maps
Portland, OR
1. Portland Hills 6.8
2. Subduction Zone 9.0

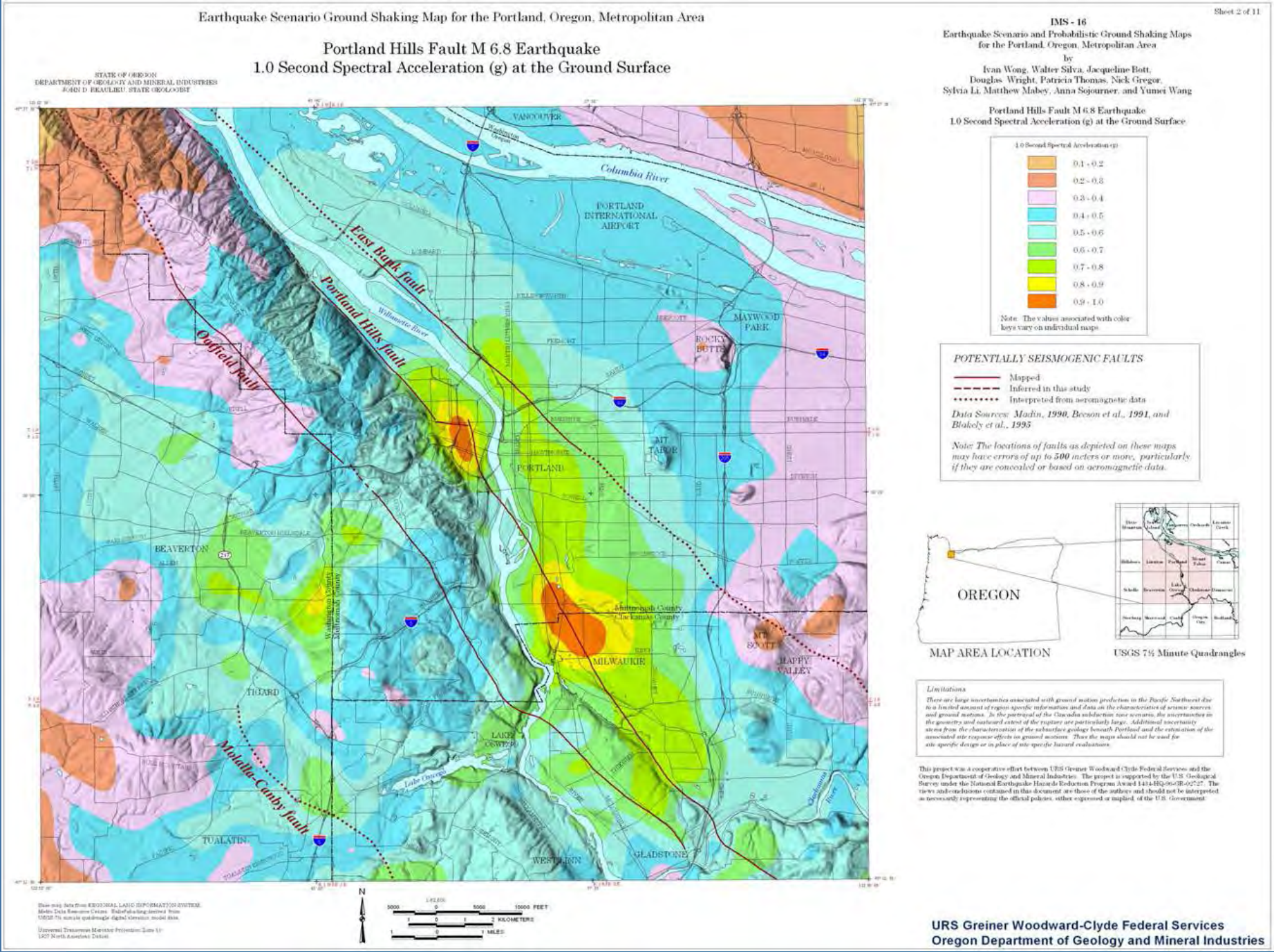

Shaking associated with a M 6.8 earthquake in Portland Hills

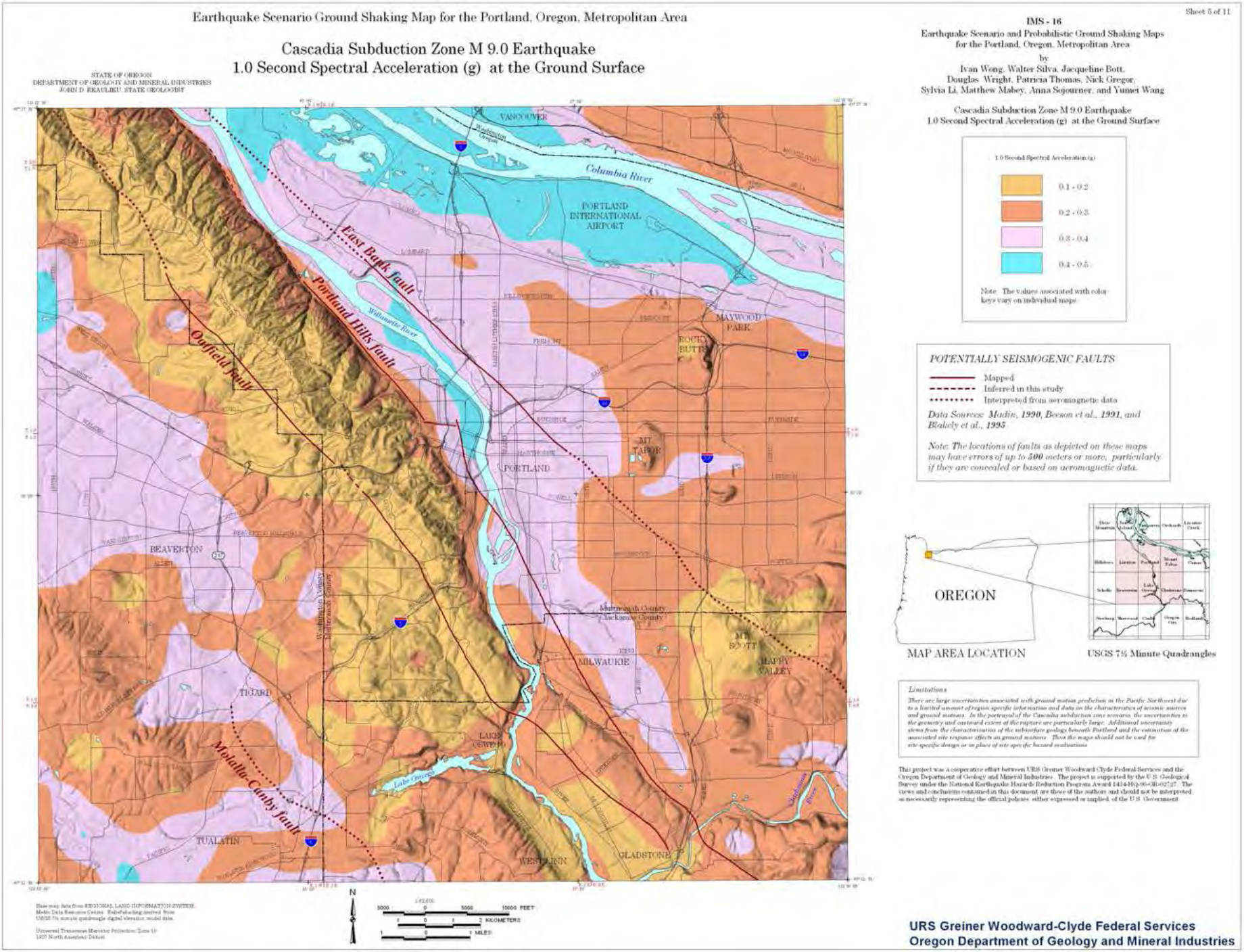

NB Shaking is one-half that of a local 6.8 earthquake